Published for SISSA by Springer

Received: *June 2, 2026*
Accepted: *August 24, 2026*
Published: *October 2, 2026*

Measurement of the cross-section for the production of a W boson in association with b-jets in pp collisions at $\sqrt{s} = 13$ TeV with the ATLAS detector



The ATLAS collaboration

Full author list at the end of the paper

E-mail: atlas.publications@cern.ch

Abstract: This paper presents a measurement of the production cross-section of a W boson associated with one or two jets, where at least one jet originates from a b-quark. The data are collected with the ATLAS detector at the LHC in proton-proton collisions at $\sqrt{s} = 13\,\text{TeV}$, corresponding to an integrated luminosity of $140\,\text{fb}^{-1}$. Differential cross-sections are presented as a function of the transverse momentum of the b-jet for both the electron and muon decay modes of the W boson. The results corrected for all detector effects are presented in a fiducial region defined with basic lepton and jet kinematics, and compared with theoretical predictions. The combined fiducial cross-section of $W + b$-jets for the electron and muon channels is measured to be 16.6 ± 1.9 pb, which is consistent with the next-to-leading-order QCD prediction of 16.8 ± 2.3 pb. The relative precision of this measurement is improved by approximately a factor of two compared with the previous ATLAS measurement at $\sqrt{s} = 7\,\text{TeV}$.

Keywords: Hadron-Hadron Scattering

ArXiv ePrint: 2605.31205

Open Access, © The Authors.
Article funded by SCOAP^3.

https://doi.org/10.1007/JHEP10(2026)027

JHEP10(2026)027

Contents

1 Introduction **1**

2 The ATLAS detector **2**

3 Data and simulated samples **3**

4 Event reconstruction and selection **4**

5 Background estimation **6**
5.1 The matrix method 6
5.2 W+jets flavour fitting 8
5.3 Estimated background contribution 9

6 Cross-section extraction **12**

7 Uncertainties **13**
7.1 Detector-level systematic uncertainties 14
7.2 Background and theoretical systematic uncertainties 14
7.3 Unfolding systematic uncertainties 15

8 Results **15**

9 Conclusions **22**

The ATLAS collaboration **28**

JHEP10(2026)027

1 Introduction

This paper presents a measurement of the cross-section for W boson production in association with one or two jets, at least one of which originates from a b-quark, in proton-proton (pp) collisions at $\sqrt{s} = 13\,\text{TeV}$. Events in which the W boson originates from a top-quark decay are excluded from the signal definition. This measurement is sensitive to heavy flavour quarks in the initial state and provides an important test of perturbative quantum chromodynamics (pQCD) in the presence of heavy quarks. In the Standard Model (SM), the dominant contribution to $W + b$-jets production arises from the splitting of a gluon into a $b\bar{b}$ pair ($W + g(\to b\bar{b})$). At next-to-leading-order (NLO), additional production mechanisms contribute, depending on the treatment of b-quark production [1].

Two commonly used approaches are the four-flavour number scheme (4FNS) and the five-flavour number scheme (5FNS), which differ in the number of active quark flavours considered in the proton parton distribution functions (PDFs). Following the notation convention of ref. [1], in the 4FNS the relevant processes include $q\bar{q}' \to Wb\bar{b}(g)$ and $gq \to Wb\bar{b}q'$, while in the 5FNS additional single b-quark processes, such as $bq \to Wbq'(g)$ and $bg \to Wbq\bar{q}'$, also contribute significantly at LHC energies [2]. A precise experimental measurement of the

$W + b$-jets production cross-section provides important input to the refinement of theoretical calculations in pQCD, as well as the validation of Monte Carlo (MC) techniques.

The $W + b$-jets process constitutes an important background to measurements of Higgs boson production, in particular in associated production modes WH and ZH with $H \to b\bar{b}$ decays [3], which are crucial for probing the coupling of the Higgs boson. The $W + b$-jets process is also an irreducible background in many searches for physics beyond the Standard Model, and in measurements of single top-quark production [4, 5].

The first measurement of the fiducial $W + b$-jets cross-section at a hadron collider was performed by the CDF Collaboration at the Tevatron with $\sqrt{s} = 1.96\,\text{TeV}$ [6]. This measurement is in tension with the corresponding NLO theoretical prediction, which lies below the data. A subsequent measurement by the D0 Collaboration [7] reported a cross-section lower than the theoretical calculation, but in agreement within theoretical uncertainties. The most recent measurement of $W + b$-jets production at the LHC was reported by the ATLAS Collaboration based on $4.6\,\text{fb}^{-1}$ of data collected in pp collisions at $\sqrt{s} = 7\,\text{TeV}$ [8]. The ATLAS measurement exceeded the NLO theoretical prediction by 1.5 standard deviations. The CMS Collaboration reported measurements of the related $W + bb$ process using 7 TeV and 8 TeV datasets, respectively [9, 10]. The measured cross-sections were found to be consistent with the NLO theoretical predictions within the experimental and theoretical uncertainties.

In this paper, the $W + b$-jets cross-section is measured using $140\,\text{fb}^{-1}$ of pp collision data collected by the ATLAS detector during the Run 2 period [11]. The W boson is reconstructed through its decay to an electron or muon, and b-jets are identified by exploiting the long lifetime and the large mass of b-hadrons. The $W + b$-jet production cross-section is measured in exclusive final states containing exactly one or exactly two reconstructed jets. The one-jet category requires exactly one reconstructed jet, which must satisfy the b-tagging requirements (referred to as b-jet in the following). The two-jet category requires exactly two reconstructed jets, of which exactly one is required to be b-tagged. Events with two or more reconstructed b-jets, as well as events with three or more reconstructed jets, are rejected in order to suppress the backgrounds from top-quark production.

2 The ATLAS detector

The ATLAS experiment [12] at the LHC is a multipurpose particle detector with a forward-backward symmetric cylindrical geometry and a near 4π coverage in solid angle.[1] It consists of an inner detector system (ID) surrounded by a thin superconducting solenoid providing a 2 T axial magnetic field, electromagnetic and hadronic calorimeters, and a muon spectrometer. The inner tracking detector covers the pseudorapidity range $|\eta| < 2.5$. It consists of silicon pixel, silicon microstrip, and transition radiation tracking detectors. Lead/liquid-argon (LAr) sampling calorimeters provide electromagnetic (EM) energy measurements with

[1] ATLAS uses a right-handed coordinate system with its origin at the nominal interaction point (IP) in the centre of the detector and the z-axis along the beam pipe. The x-axis points from the IP to the centre of the LHC ring, and the y-axis points upwards. Polar coordinates (r, ϕ) are used in the transverse plane, ϕ being the azimuthal angle around the z-axis. The pseudorapidity is defined in terms of the polar angle θ as $\eta = -\ln\tan(\theta/2)$ and is equal to the rapidity $y = \frac{1}{2}\ln\left(\frac{E+p_z}{E-p_z}\right)$ in the relativistic limit. Angular distance is measured in units of $\Delta R \equiv \sqrt{(\Delta\eta)^2 + (\Delta\phi)^2}$.

JHEP10(2026)027

high granularity within the region $|\eta| < 3.2$. A steel/scintillator-tile hadronic calorimeter covers the central pseudorapidity range ($|\eta| < 1.7$). The endcap and forward regions are instrumented with LAr calorimeters for EM and hadronic energy measurements up to $|\eta| = 4.9$. The muon spectrometer surrounds the calorimeters and is based on three large superconducting air-core toroidal magnets with eight coils each. The field integral of the toroids ranges between 2.0 and 6.0T m across most of the detector. The muon spectrometer includes a system of precision tracking chambers up to $|\eta| = 2.7$ and fast detectors for triggering up to $|\eta| = 2.4$. The luminosity is measured mainly by the LUCID-2 [13] detector that is located close to the beampipe. A two-level trigger system is used to select events [14]. The first-level trigger is implemented in hardware and uses a subset of the detector information to accept events at a rate close to 100 kHz. This is followed by a software-based trigger that reduces the accepted rate of complete events to 1.25 kHz on average depending on the data-taking conditions.

3 Data and simulated samples

The data used in this analysis were collected with the ATLAS detector between 2015 and 2018 in pp collisions at $\sqrt{s}$ =13 TeV. The corresponding total integrated luminosity is 140 fb^{-1} with a relative uncertainty of 0.83% [11]. Data quality requirements are applied to ensure that all relevant detector subsystems were operating under stable and optimal conditions. Data events are collected using single-electron or single-muon triggers [15, 16]. The lowest p_{T} threshold of the muon triggers is 26 GeV, while the lowest transverse energy (E_{T}) threshold used for the electron trigger is 24 GeV for the 2015 data-taking period and was raised to 26 GeV in subsequent years to accommodate the increasing LHC instantaneous luminosity.

Monte Carlo events with full detector simulation are used to model signal and most background processes. For inclusive W boson production in association with both light- and heavy-flavour jets, two sets of fully simulated samples are used, comprising all leptonic decays $W \to \ell\nu$ ($\ell = e, \mu, \tau$). One set is produced using the Sherpa v2.2.11 [17] ATLAS configuration [18] that performs explicit matrix element (ME) calculations of 0–2 partons at NLO and 3–5 partons at leading order (LO). The PDF set used for event generation is NNPDF 3.0 NNLO [19] with $\alpha_S = 0.118$. The other set is generated using MadGraph5_aMC@NLO [20] for W+0–3 partons at NLO accuracy, merged with the FxFx procedure [21], and interfaced to Pythia (v8.245) [22] for parton showering and hadronisation using the A14 tune [23] (MGaMC+Py8 FxFx). For this sample, the NNPDF 3.1 LUXQED NNLO [24] PDF set is used, also with $\alpha_S = 0.118$. Both signal samples for the W+jets process are based on the 5FNS. The Sherpa sample is used for the nominal measurement while the MGaMC+Py8 FxFx sample is employed for cross-checks and for the evaluation of modelling uncertainties.

For W+jets MC samples, events are further categorised according to the flavour of the hadron associated with the jet. At particle-level, jets are classified as b-, c-, or light-jets using a cone-based matching procedure. Jets are labelled as b-jets if they are found within $\Delta R = 0.3$ of at least one b-hadron with $p_{\mathrm{T}} > 5$ GeV. In cases where a b-hadron is matched to more than one jet, only the jet closest in ΔR is labelled as a b-jet. Jets not identified as b-jets are subsequently labelled as c-jets if they are within $\Delta R = 0.3$ of any c-hadron with $p_{\mathrm{T}} > 5$ GeV. All remaining jets are classified as light-jets. Simulated events are then classified sequentially

JHEP10(2026)027

as $W+b$-jets or $W+c$-jets according to whether the leading (highest p_{T}) heavy-flavour jet is a b- or c-jet, respectively. Events containing only light-jets are classified as W+light-jets.

The Z+jets processes are simulated with Sherpa v2.2.11 using the same configuration as for W+jets. The top quark processes, including $t\bar{t}$ and single top in the tW, s- and t-channels, are simulated at NLO using the Powheg Box v2 [25–28] generator and interfaced to Pythia (v8.230) for showering and hadronisation using the A14 tune. The $t\bar{t}$ sample is further reweighted to match the NNLO QCD (+ NLO EW) differential calculation [29]. The diboson (VV, V=W, Z) processes, where one vector boson decays leptonically and the other decays hadronically, are simulated using Sherpa v2.2.1 [17], with NLO MEs for up to one parton emission and LO MEs for two or three parton emissions.

The generated samples are processed using the Geant4-based ATLAS detector simulation [30, 31] and the same reconstruction algorithms are applied to simulated and recorded data. To account for pile-up, multiple overlaid inelastic pp collisions are simulated with Pythia (v8.186) using the A3 tune [32] and the NNPDF 2.3 LO PDF [33]. The distribution of the average number of interactions per bunch crossing in the simulations is weighted to reflect the one in data. Simulated events are then corrected for known differences between data and simulation in reconstruction and identification efficiencies, and in energy and momentum scales and resolutions.

4 Event reconstruction and selection

Candidate $W+b$-jets events are required to have exactly one high-p_{T} electron or muon, as well as missing transverse momentum consistent with the presence of a neutrino from the W boson decay, and one or two reconstructed jets, exactly one of which must be identified as a b-jet. All events must have at least one reconstructed vertex formed by the intersection of at least two tracks with $p_{\mathrm{T}} > 500\,\mathrm{MeV}$. In events with multiple vertices, the vertex with the largest Σp_{T}^2 of the associated tracks is taken to be the primary hard-scatter vertex (PV).

Electron candidates are required to satisfy $E_{\mathrm{T}} > 28\,\mathrm{GeV}$ and $|\eta| < 2.47$, excluding the calorimeter transition region $1.37 < |\eta| < 1.52$. They are reconstructed by matching topological energy clusters in the electromagnetic calorimeter with inner-detector tracks. Electron identification employs a likelihood discriminant that combines calorimeter shower shapes, tracking and cluster-track matching quantities. The "Tight" identification working point [34] is used to maximise the rejection of background from misidentified objects. Additional requirements are imposed on the electron tracks: the longitudinal impact parameter (z_0) is required to satisfy $|z_0 \sin\theta| < 0.5$ mm, where θ is the angle of the track with respect to the beam-line, and the transverse impact parameter significance (d_0/σ_{d_0}) is required to satisfy $|d_0/\sigma_{d_0}| < 5$. Electrons must also fulfil the "PLImprovedVeryTight" isolation criterion [35] that significantly suppresses background from photons or hadrons misidentified as electrons and non-prompt electrons from the decay of heavy-flavour hadrons.

Muon candidates are selected in the region $|\eta| < 2.5$ and are required to have $p_{\mathrm{T}} > 28\,\mathrm{GeV}$. They are identified by matching ID tracks from the PV to either full tracks or track segments reconstructed in the muon spectrometer. Muons are required to satisfy the "Tight" identification working point [36], based on quality criteria applied to the inner-detector and muon-spectrometer tracks. In addition, the longitudinal impact parameter of

JHEP10(2026)027

the muon track is required to satisfy $|z_0 \sin\theta| < 0.5$ mm, and the transverse impact parameter significance is required to satisfy $|d_0/\sigma_{d_0}| < 3$. Muons must also be isolated, passing the "Tight_VarRad" working point [36], which is built from tracking and calorimeter information, with a p_{T}-dependent variable cone.

The presence of a neutrino in the W boson decay is inferred from the missing transverse momentum. It is computed as the negative vector sum of the transverse momenta of all identified physics objects and an additional soft term. The soft term is constructed from all tracks that are associated with the primary vertex, but not associated with any selected physics object [37]. In this analysis, the magnitude of missing transverse momentum ($E_{\mathrm{T}}^{\mathrm{miss}}$) is required to satisfy $28\,\mathrm{GeV} < E_{\mathrm{T}}^{\mathrm{miss}} < 60\,\mathrm{GeV}$. The upper bound provides effective suppression of backgrounds from top-quark production. Jets are reconstructed using the anti-k_t algorithm [38] with a radius parameter $R = 0.4$, as implemented in the FastJet package [39]. The inputs to this algorithm are particle flow (PFlow) objects [40], which combine measurements from the ATLAS inner detector and calorimeters to improve the jet energy resolution and increase the jet reconstruction efficiency. Jets are calibrated using a simulation-based calibration scheme, followed by in situ corrections to account for differences between simulation and data [41]. To suppress jets originating from pile-up interactions, jets with $p_{\mathrm{T}} < 60\,\mathrm{GeV}$ and $|\eta| < 2.4$ are required to have a significant fraction of constituent tracks originating from the PV, as defined by a jet vertex tagger (JVT) discriminant [42]. Selected jets must have $p_{\mathrm{T}} > 25\,\mathrm{GeV}$ and $|\eta| < 2.5$.

At reconstruction level, b-jets are identified using the DL1r b-tagging discriminant [43]. DL1r is a deep neural network that takes as input the outputs of several lower-level taggers, including track impact parameter significance, secondary vertex likelihood, and a recurrent neural network capturing track correlations within a jet. It then combines these features to produce a single discriminant that significantly improves b-jet identification over previous boosted decision tree based taggers. The 60% tagging-efficiency working point is used, corresponding to a 60% selection efficiency for particle-level b-jets, with rejection rates of 40 against c-jets and 2500 against light-jets. This stringent working point is chosen to effectively suppress the large background from $W + c$/light-jets. Selected b-jets must satisfy $p_{\mathrm{T}} > 25\,\mathrm{GeV}$ and $|\eta| < 2.5$.

To avoid the double-counting of detector signatures, an overlap-removal procedure is applied to uniquely identify the objects in an event. Jets within $\Delta R < 0.2$ of a selected lepton are removed if they are likely to originate from the lepton or a radiated photon. Subsequently, leptons within $\Delta R = 0.4$ of any remaining jet are discarded, as they are potential decay products of heavy quarks in the jet.

Signal events are selected by requiring exactly one lepton, $28\,\mathrm{GeV} < E_{\mathrm{T}}^{\mathrm{miss}} < 60\,\mathrm{GeV}$, and a transverse mass $m_{\mathrm{T}} = \sqrt{2p_{\mathrm{T}}^{\ell} E_{\mathrm{T}}^{\mathrm{miss}}(1 - \cos(\Delta\phi))} > 65\,\mathrm{GeV}$, where $\Delta\phi$ is the azimuthal angle between the lepton and the missing transverse momentum. Events are further required to contain one or two reconstructed jets, exactly one of which must be b-tagged. The selected events are categorised into two exclusive signal regions:

- `1j1b` category: exactly one jet in the event, and it passes the b-jet requirement;

JHEP10(2026)027

- `2j1b` category: exactly two jets in the event, and only one of them passes the b-jet requirement.

This categorisation facilitates a better control of backgrounds, thereby reducing uncertainties in the final measurement. Due to the selection of central jets with high transverse momentum (p_{T}) and the use of the tight b-tagging working point, the majority of the $W + b$-jet events with two particle-level b-jets are reconstructed as events with one b-jet candidate. As a result, although the measurement is performed using reconstructed events with only one b-jet, it remains sensitive to the production of $W + b$-jets with two particle-level b-jets, and is therefore unfolded to the fiducial region with one or two b-jets, as described in section 6.

5 Background estimation

After event selection, the signal purity is approximately 30% for both electron and muon channels. Several processes can mimic the signal and contribute to the overall background. The major background comes from $W + c$-jets and $W+$ light-jets. These events contain a genuine lepton from the W boson decay and a jet that is misidentified as a b-jet, originating from either a c-quark or a light-flavour quark or gluon. They exhibit kinematics nearly identical to the signal and can be distinguished only by examining the distribution of the b-tagger response. As these processes are not modelled with sufficient accuracy by MC simulation, their contributions are estimated by using a data-driven technique referred to as the flavour-fit method [44].

Additional background contributions arising from single-top, $t\bar{t}$, and diboson processes also play an important role. These backgrounds include both a real lepton and a real b-jet in their final state. Considering that these processes are usually well modelled by simulation, their contributions are directly evaluated with fully simulated MC samples. Since $t\bar{t}$ and single top events contribute notably in the high b-jet p_{T} region, dedicated top control regions are constructed to validate the MC modelling, and good agreement is observed. Another type of background comes from multijet production, where one of the jets is either misidentified as a lepton, or contains a non-prompt lepton produced in the decay of a heavy-quark. A data-driven method named the "matrix method" [45] is applied to evaluate the multijet contribution. The Z+jets process also contributes to the selected events, primarily when one lepton from the Z boson decay is not reconstructed and a b-jet is present in the final state. The Z+jets contribution is much smaller compared with W+jets or top processes, and is quantified using MC simulations. The $W(\to \tau\nu)$+jets process is also treated as a background and estimated using MC simulations, contributing only around 1% of the total event yields.

5.1 The matrix method

The matrix method is a widely used technique to estimate backgrounds containing non-prompt or misidentified ("fake") leptons. The goal of the matrix method is to estimate the number of events in the data sample with a prompt ("real") lepton (N_R) and events with a "fake" lepton (N_F).

JHEP10(2026)027

Two event selection criteria are defined for leptons based on their isolation quality requirement:

- "Tight" events satisfy the nominal selection and N_T corresponds to the number of events passing such requirements.
- "Anti-Tight" events satisfy the nominal selection, except that the leptons are required to fail the nominal isolation criteria while passing a very loose track-based isolation requirement, in order to avoid using objects that are significantly different from the signal selection. The number of such events is denoted by $N_{!T}$.

Since the probabilities for real and fake leptons to satisfy the Tight selection differ, the number of fake-lepton events in the signal region can be determined from the observed number of data events passing each set of selection criteria. The fake-lepton contribution is obtained by solving a system of linear equations that relates these event counts to the efficiencies for real and fake leptons to pass the Tight and Anti-Tight selections:

$$\begin{pmatrix} N_{\mathrm{T}} \\ N_{!\mathrm{T}} \end{pmatrix} = \begin{pmatrix} r & f \\ 1-r & 1-f \end{pmatrix} \begin{pmatrix} N_{\mathrm{R}} \\ N_{\mathrm{F}} \end{pmatrix}. \tag{5.1}$$

In the equation, r and f represent the efficiencies of passing the Tight selection for real and fake leptons, respectively. MC simulated signal samples, which are corrected to data as in section 3, are used to derive the efficiency parameter r. Events are required to satisfy the signal region kinematic selection and the selected lepton must be matched to a particle-level lepton. The fake-lepton efficiency f, however, is measured in a region enriched in non-prompt and misidentified leptons, referred to as the fake control region, which is defined by reversing the $E_{\mathrm{T}}^{\mathrm{miss}}$ and m_{T} requirements used for the signal event selection: $E_{\mathrm{T}}^{\mathrm{miss}} < 28$ GeV and $m_{\mathrm{T}} < 40\,\mathrm{GeV}$. All other requirements used for signal selection are kept for the fake control region construction. Any residual contribution from prompt leptons (such as W+jets, $t\bar{t}$ and diboson) is then subtracted using MC simulated samples. Both efficiencies r and f are determined as functions of the lepton p_{T} and η, and are evaluated separately for the `1j1b` and `2j1b` signal regions.

The uncertainties associated with the matrix method are evaluated by considering systematic effects on the "real" and "fake" lepton efficiency measurements. The uncertainties of r include: signal modelling, evaluated with the difference between the r-values obtained using Sherpa and MGaMC+Py8 FxFx signal samples mentioned in section 3, experimental uncertainties propagated to the r calculation; and the statistical uncertainty.

The uncertainties associated with the fake-lepton efficiency f account for the choice of the fake control region and uncertainties propagated from the prompt-lepton subtraction. The impact of the fake control region definition is evaluated using two alternative configurations. In the first configuration, the kinematic criteria used to construct the fake control regions are modified. The $E_{\mathrm{T}}^{\mathrm{miss}}$ requirement is inverted from $E_{\mathrm{T}}^{\mathrm{miss}} < 28$ GeV to a "signal-like" region with $E_{\mathrm{T}}^{\mathrm{miss}} > 28\,\mathrm{GeV}$, while the m_{T} requirement is retained to ensure orthogonality with the signal region. The matrix method is reapplied, and the deviation from the nominal value is assigned as an uncertainty. Given the dependence of the "fake" efficiency on jet flavour,

JHEP10(2026)027

which may be different between the fake control region and the signal region, in the second configuration the b-jet identification threshold in the fake control region is relaxed from a 60% tagging efficiency working point to a 70% tagging efficiency working point in order to modify the jet flavour composition. The matrix method is repeated, and the resulting difference from the nominal multijet background estimate is taken as an additional uncertainty. To evaluate the impact of the prompt-lepton subtraction, both experimental and theoretical uncertainties are considered for the MC samples used in the prompt-lepton subtraction and are propagated to the final multijet estimation. The total uncertainties in the multijet background estimation are approximately 70% (85%) in the electron channel, and 45% (50%) in the muon channel for the `1j1b` (`2j1b`) region, with the dominant contribution arising from the variation in the $E_{\mathrm{T}}^{\mathrm{miss}}$ requirement.

5.2 W+jets flavour fitting

The $W + c$-jets and $W+$ light-jets processes constitute the dominant backgrounds in this analysis, exhibiting nearly identical kinematics to the signal. Their contributions, along with the signal $W + b$-jets process, are extracted simultaneously using a χ^2 fit to the b-tagging discriminant (DL1r tagging score) distribution. This procedure is referred to as the flavour-fit method in the following.

With the 60% efficiency working point used for the b-jet selection, events are further divided into two bins depending on the DL1r tagging score of the selected b-jet: the 20–60% tagging-efficiency bin and the 0–20% tagging-efficiency bin. To extract the signal event yields in the data, a χ^2 is defined as follows:

$$\chi^2 = \sum_{i}^{N_{\mathrm{bins}}} \frac{(N_i^{\mathrm{data}} - p_0 \cdot N_i^{\mathrm{MC,W+b}} - p_1 \cdot N_i^{\mathrm{MC,W+j}} - N_i^{\mathrm{MC,other}})^2}{\sigma_{\mathrm{data}}^2 + \sigma_{\mathrm{MC}}^2}. \tag{5.2}$$

Here N_i^{data} is the number of data events in the ith bin and $N_i^{\mathrm{MC,W+b}}$ is the number of signal events in the ith bin from MC simulation. The $W + c$-jets and $W+$ light-jets events are grouped together, denoted by $N_i^{\mathrm{MC,W+j}}$, given that their contributions in the 0–20% tagging bin are very small, and all other background events are similarly combined to $N_i^{\mathrm{MC,other}}$. The scale factors, p_0 and p_1, are free parameters that can be determined analytically from the data to extract the observed $W + b$-jets signal and combined $W + c$-jets and $W+$ light-jets background (denoted by $W+$ other-jets in the following text). The uncertainties of data or MC (σ_{data} and σ_{MC}) do not affect the solution of this linear system. The flavour-fit procedure is performed inclusively for the total cross-section measurement, and independently in each b-jet p_{T} bin for the differential cross-section measurement.

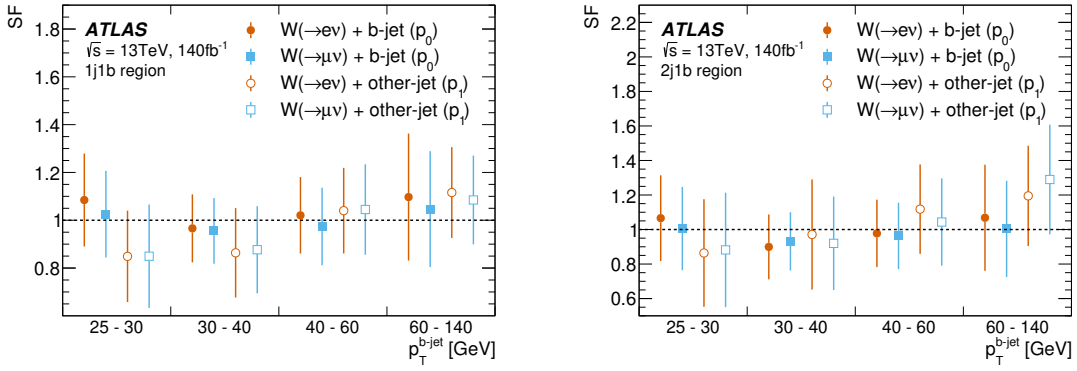
Jet-flavour-dependent DL1r calibrations are applied to correct for differences in tagging efficiencies between data and simulation before the flavour fit. For the $W + b$-jets signal, corrections are derived separately in the two tagging bins following standard ATLAS procedures [46]. For the $W + c$-jets and $W+$ light-jets backgrounds, the 0–60% correction factors from ATLAS standard recommendations [47, 48] are applied in both regions. To account for the potential differences in the correction factors in the 0–20% region, an additional 100% uncertainty is assigned.

The inclusive fit results for signal and $W+$ other-jets are summarised in table 1. The statistical uncertainties on the fitted parameters p_0 and p_1 are estimated with the bootstrap

JHEP10(2026)027

Type	e 1j1b	e 2j1b	μ 1j1b	μ 2j1b
$W+b$-jets (p_0)	$1.02 \pm 0.01 \pm 0.16$	$0.99 \pm 0.01 \pm 0.21$	$0.99 \pm 0.01 \pm 0.15$	$0.97 \pm 0.01 \pm 0.19$
$W+$ other-jets (p_1)	$0.93 \pm 0.01 \pm 0.17$	$1.04 \pm 0.01 \pm 0.26$	$0.93 \pm 0.01 \pm 0.18$	$1.02 \pm 0.01 \pm 0.26$

Table 1. Fitted scale factors for $W+b$-jets and $W+$ other-jets in the 1j1b and 2j1b regions for both electron and muon final states. The quoted uncertainties correspond to the statistical (first) and systematic (second) components.



(a) (b)

Figure 1. Fitted scale factors (SF) for $W+b$-jets (p_0) and $W+$ other-jets (p_1) in bins of b-jet p_{T} in the (a) 1j1b and (b) 2j1b regions. The error bars represent the total uncertainty.

method [49]. One thousand replicas are generated for both data and simulated spectra based on their statistical uncertainties, and the fit is conducted for each replica. The standard deviation of the fitted parameters of all replicas is quoted as the statistical uncertainty. Systematic uncertainties on the fitted parameters are evaluated using an offset method. This method reruns the fit while varying only one systematic source at a time, and iterates through all systematic sources. For each variation, the fitted parameters are extracted, and the deviation from the nominal value is assigned as the systematic uncertainty. An additional systematic uncertainty is evaluated to account for differences between Sherpa and MGaMC+Py8 FxFx in modelling $W+$jets production. This uncertainty is incorporated by substituting the DL1r score shape of $W+$jets from one generator with the other during the flavour fitting procedure. For the $W+b$-jets signal process, in both 1j1b and 2j1b signal regions, and for both electron and muon final states, the dominant systematic uncertainties on the fitted parameters arise from $W+$jets theoretical uncertainties and b-tagging calibration. Similarly, for the $W+$ other-jets process, the dominant systematic uncertainties on the fitted parameters arise from b-tagging calibration.

For differential measurement, independent fits are conducted in four bins of b-tagged jet p_{T}: 25–30 GeV, 30–40 GeV, 40–60 GeV and 60–140 GeV. The fitting strategy and uncertainty evaluation are identical to those used for the inclusive measurement. The fitted scale factors are shown in figure 1.

5.3 Estimated background contribution

The expected numbers of events for all processes after the previous background estimation are summarised in table 2. In the table, $W+b$, $W+c$ and $W+$ light-jet contributions are

JHEP10(2026)027

Type	e 1j1b	e 2j1b	μ 1j1b	μ 2j1b
$W+b$-jet	180100 ± 800	159800 ± 600	236400 ± 800	206900 ± 600
$W+c$-jet	195000 ± 1000	90600 ± 600	248000 ± 1000	110800 ± 700
$W+$ light-jet	19700 ± 700	10500 ± 400	32000 ± 2000	17000 ± 1000
$W \to \tau\nu$	4500 ± 300	3200 ± 200	5500 ± 300	4000 ± 200
Z+jet	23200 ± 200	26100 ± 200	44100 ± 700	27800 ± 400
Diboson	2100 ± 20	3150 ± 30	2610 ± 20	3800 ± 30
Single top	69000 ± 90	88400 ± 100	81900 ± 100	101000 ± 100
$t\bar{t}$	25340 ± 70	121000 ± 200	29900 ± 80	138200 ± 200
Multijet	17000 ± 12000	15000 ± 13000	20000 ± 9000	20000 ± 10000
Total prediction	536000 ± 1000	517000 ± 1000	700000 ± 3000	627000 ± 2000
Data	535566	517204	699516	627216

Table 2. Observed and expected number of events in each signal region after the flavour fit. Only MC statistical uncertainties are shown for the V+jets, diboson and top-quark processes, as well as the total predictions. For the multijet process, the total uncertainty is displayed instead.

separated according to the particle-level flavour of the b-tagged jet as explained in section 3, and their event yields are corrected by the flavour fitting. The corrected b-jet p_{T} distributions are shown in figure 2, demonstrating the contribution from each process.

JHEP10(2026)027

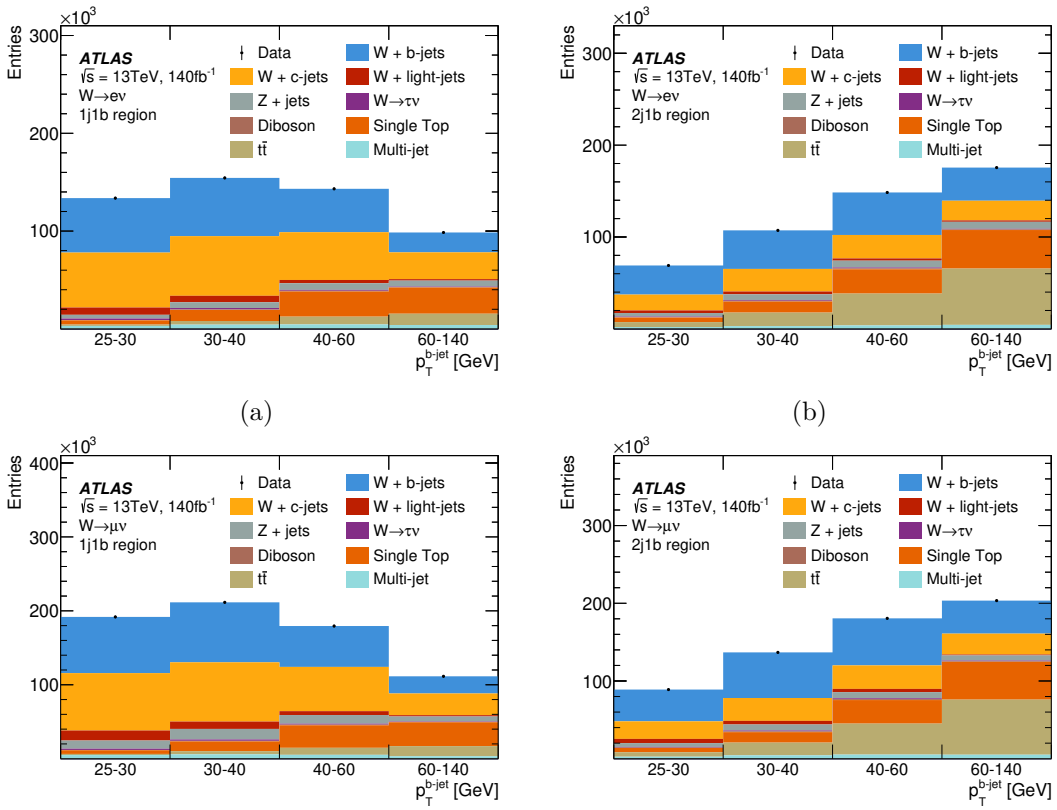


Figure 2. b-jet p_{T} distribution after the flavour fit for the (a) electron `1j1b`, (b) electron `2j1b`, (c) muon `1j1b` and (d) muon `2j1b` regions.

JHEP10(2026)027

Requirement	Cut	
Lepton transverse momentum	$p_{\mathrm{T}} > 28$ GeV	
Lepton pseudo-rapidity	$\lvert\eta\rvert < 2.5$	
Neutrino	$p_{\mathrm{T}} > 20$ GeV	
m_{T}	$m_{\mathrm{T}} > 40$ GeV	
Jet transverse momentum	$p_{\mathrm{T}} > 25$ GeV	
Jet rapidity	$\lvert y\rvert < 2.5$	
Jet multiplicity	$n = 1$	$n = 2$
b-jet multiplicity	$n_b = 1$	$n_b \geq 1$
Jet isolation	$\Delta R(\ell, \mathrm{jet}) > 0.4$	

Table 3. Definition of the particle-level fiducial region of the measurement.

6 Cross-section extraction

The $W + b$-jets yields obtained from the flavour fits are converted into a fiducial cross-section for $W + b$-jets production times branching ratio for a single leptonic decay channel ($W \to \ell\nu$) by correcting for all detector effects using MC simulation. The particle-level fiducial region is defined in table 3. At particle-level, objects are selected using requirements closely matching the reconstruction-level selection described in section 4 in order to minimize the dependence of the measurement on theoretical predictions. In this definition, the lepton kinematic variables are computed using final-state leptons (electrons or muons) originating from the W boson decay, excluding electrons or muons from τ-lepton decays. Photons radiated within a cone of $\Delta R = 0.1$ around the direction of a final-state lepton are added to the lepton four-momentum. The resulting object is referred to as a 'dressed' lepton. Particle-level jets are reconstructed from generated events without detector simulation. They are clustered using the anti-k_t algorithm [38] with a radius parameter $R = 0.4$. All detector-stable particles with a lifetime τ satisfying $c\tau > 10$mm are used, excluding those expected to deposit little or no energy in the calorimeters (i.e., muons and neutrinos). Particle-level jets are classified as b-jets using procedure described in section 3. Particle-level selections on neutrino p_{T} and m_{T} are looser than the reconstruction-level variants due to the large experimental resolution in these quantities. The fraction of selected particle-level events that fail the reconstructed $E_{\mathrm{T}}^{\mathrm{miss}}$ requirement is around 25%.

For the inclusive measurement, two truth (particle-level) jet regions are defined for the unfolding procedure: the one-jet region (requiring one truth b-jet) and the two-jet region (requiring at least one truth b-jet). For the differential measurement, each truth region is further subdivided into four truth b-jet p_{T} bins: 25–30 GeV, 30–40 GeV, 40–60 GeV, and 60–140 GeV. If two b-jets are present in an event, the leading b-jet (higher p_{T}) is used for the differential measurement. The differential measurement is not extended to higher b-jet p_{T} because of the background contamination from top processes.

JHEP10(2026)027

The unfolding procedure can be expressed as the following formula:

$$\sigma_i = \frac{\sum_j A^{-1}_{i,j} \cdot f_j \cdot (d_j - b_j)}{L \cdot e_i}, \tag{6.1}$$

where the factors are defined as:

- σ_i: unfolded cross-section in i-th bin in b-jet p_{T} or jet multiplicity.
- $d_j - b_j$: background-subtracted data event number in j-th bin.
- L: integrated luminosity.
- Response matrix A: bin-to-bin migrations between the reconstructed and the truth distribution.
- Efficiency correction factors $e_i = N^{RT_i}/N^{T_i}$: the ratio of truth-reco-matched events (N^{RT_i}) to truth events (N^{T_i}) in the i-th bin.
- Fiducial correction factors $f_j = N^{R_jT}/N^{R_j}$: the ratio of truth-reco-matched events (N^{R_jT}) to reco events (N^{R_j}) in the j-th bin.

The Monte Carlo sample simulated with Sherpa is used to derive the efficiency correction factors e_i, the fiducial correction factors f_j, and the response matrix $A_{i,j}$. Alternative results are also obtained with MGaMC+Py8 FxFx and serve as an estimation of modelling uncertainty. For the inclusive measurement, the matrix inversion is conducted straightforwardly, since there are only two bins in the jet multiplicity and the migration effect is small. For the differential measurement, there are eight bins in total (two jet multiplicity bins $\times$ four $p_{\mathrm{T}}^{\text{b-jet}}$ bins), and the response matrix is inverted using an iterative Bayesian technique [50] to account for the low purity, mostly due to the resolution in the $p_{\mathrm{T}}^{\text{b-jet}}$ measurement. In the Bayesian unfolding procedure, the MC prediction is used as the initial prior, and five successive iterations are performed to suppress the bias from the initial distribution. The modelling uncertainties and the potential unfolding bias will be discussed in section 7.

7 Uncertainties

Uncertainties in the $W + b$-jets cross-section measurements arise from both statistical effects associated with the finite size of the analysed data and systematic effects related to detector-level selection, background determination, theoretical predictions and the unfolding method. Uncertainties are treated as correlated, when appropriate, between lepton channels, signal and background processes and across observables. Some uncertainty sources can affect multiple components of this analysis; these are evaluated by repeating the full analysis under each systematic variation, and taking the difference between the nominal result and the varied result as the uncertainty. The total systematic uncertainties on the final unfolded cross-sections are obtained by summing in quadrature all individual contributions.

JHEP10(2026)027

7.1 Detector-level systematic uncertainties

Detector-related systematic uncertainties are defined as uncertainties arising from the selection or calibration of the physics objects entering the measurement and from the luminosity measurement. They are derived by propagating each systematic shift from each systematic source through both the flavour fit and the unfolding inputs (response matrices, efficiency correction factors, and fiducial correction factors) into the unfolded data.

Systematic uncertainties on the leptons are related to the trigger, reconstruction, identification and isolation criteria adopted in the selection of electrons and muons [35, 36]. Variations in the electron energy scale and resolution are taken into account, as are those related to the muon momentum scale, the inner-detector and muon spectrometer resolution, and the sagitta-bias corrections. These uncertainties are specific for each leptonic final state and are therefore treated as uncorrelated between the two lepton channels.

The uncertainties associated with the reconstructed jets take into account corrections to the energy scale and resolution [41]. They are evaluated by scaling and smearing the jet four-momentum in the simulation according to the calibration uncertainties. The uncertainty in the JVT efficiency is also included. The systematic uncertainty on $E_{\mathrm{T}}^{\mathrm{miss}}$ accounts for the energy scale and resolution of the soft hadronic activity in the event [37].

Uncertainties related to flavour tagging are derived from the calibration of the DL1r tagger using data control samples enriched in b- [46], c- [48], or light-jets [47], covering jet transverse momenta up to several hundred GeV. Discrepancies in flavour-tagging efficiencies between data and simulation are corrected in simulation as a function of jet flavour, b-tagging discriminant thresholds, and jet p_{T}. In the uncalibrated 0–20% efficiency region for c- and light-jets, an additional 100% uncertainty is assigned to cover the potential differences in the correction factors. The uncertainties in the flavour-tagging calibration are extrapolated to high p_{T} using MC simulation [51].

The uncertainty in the combined 2015–2018 integrated luminosity is 0.83% [11], obtained using the LUCID-2 detector for the primary luminosity measurements [13].

7.2 Background and theoretical systematic uncertainties

In addition to detector effects, uncertainties from imperfect MC modelling are included for both signal and background processes. For top quark processes, the modelling uncertainties considered in this analysis include variations in NLO matching, parton shower, initial- and final-state radiation, and resummation damping. The theoretical uncertainties due to missing higher-order corrections are probed by variations of the QCD scales, the PDF set, and α_S. These effects are evaluated using alternative MC samples or modified parameter values following standard ATLAS prescriptions [52].

Theoretical uncertainties due to missing higher-order corrections in V+jets production arise from two main sources. The scale uncertainties are determined by varying independently the QCD renormalisation (μ_R) and factorisation (μ_F) scales by a factor of 0.5 or 2 with an additional constraint of $0.5 \leq \mu_R/\mu_F \leq 2$. The envelope of the varied predictions is taken as the error estimate, commonly referred to as the "7-point uncertainty". Effects due to PDF uncertainties are also considered and follow the recipes provided by the NNPDF group [19].

JHEP10(2026)027

For signal W + b-jet processes, an additional modelling uncertainty is considered by comparing Sherpa and MGaMC+Py8 FxFx generators. This variation affects both the flavour fitting and the unfolding procedure. The impact of this modelling uncertainty is evaluated by repeating the full analysis using the MGaMC+Py8 FxFx samples and taking the difference with respect to the nominal Sherpa-based result.

The estimations of uncertainties associated with the multijet background and with the W + c-jets and W+ light-jets backgrounds are described in section 5.1 and section 5.2, respectively.

7.3 Unfolding systematic uncertainties

Uncertainties in the unfolding procedure arise from the statistical uncertainty of Sherpa signal MC samples, from the modelling uncertainties of the Sherpa signal samples, and from the intrinsic bias of the unfolding method associated with the prior used in the Bayesian unfolding procedure.

The impact of the finite simulated sample size is evaluated using 1000 pseudo-experiments, in which the unfolding inputs are fluctuated independently according to Gaussian distributions and the standard deviation of the results is adopted as the uncertainty estimate.

Signal theoretical uncertainties arising from missing higher-order corrections and other modelling uncertainties can affect response matrices, efficiency correction factors and fiducial correction factors. These uncertainties are evaluated using QCD scale and PDF variations in the Sherpa W+jet sample, as well as by comparing the unfolded results with those obtained using MGaMC+Py8 FxFx.

The dependence of the Bayesian unfolding regularisation procedure on the choice of the initial prior is determined by reweighting the generator-level distribution of $p_{\mathrm{T}}^{\text{b-jet}}$ in the Sherpa samples to provide a better description of the data at detector level. The reweighted samples are treated as pseudo-data and unfolded using the nominal response matrix, and the observed deviation from the reweighted generator-level distribution is quoted as the unfolding bias introduced by the regularisation.

The statistical uncertainty of the data is propagated through the unfolding by using 1000 pseudo-experiments. The flavour fit and the unfolding are repeated for each data replica.

8 Results

The unfolded results for the inclusive $W + b$-jets cross-section and the differential cross-section $\mathrm{d}\sigma/\mathrm{d}p_{\mathrm{T}}^{\text{b-jet}}$ are shown in figure 3. The results are compared with the predictions of two event generators, Sherpa and MGaMC+Py8 FxFx (see section 3). The uncertainties on the theory predictions are from scale and PDF variations, as described in section 7. The dominant uncertainties are due to scale variations, which are about 10% for both generators. The PDF uncertainties are smaller, at the level of 1–2%. Statistical uncertainties from the finite size of the simulated samples are negligible on the theory predictions.

For the final results, the total fiducial cross-sections and the differential cross-sections in each analysis region are combined across the electron and muon channels using the Best Linear Unbiased Estimate (BLUE) method [53]. The χ^2/N_{dof} summed over `1j1b` and `2j1b` regions, or the equivalent log likelihood $-2\log\mathcal{L}$ following the definition in ref. [54], are 0.2/2

JHEP10(2026)027

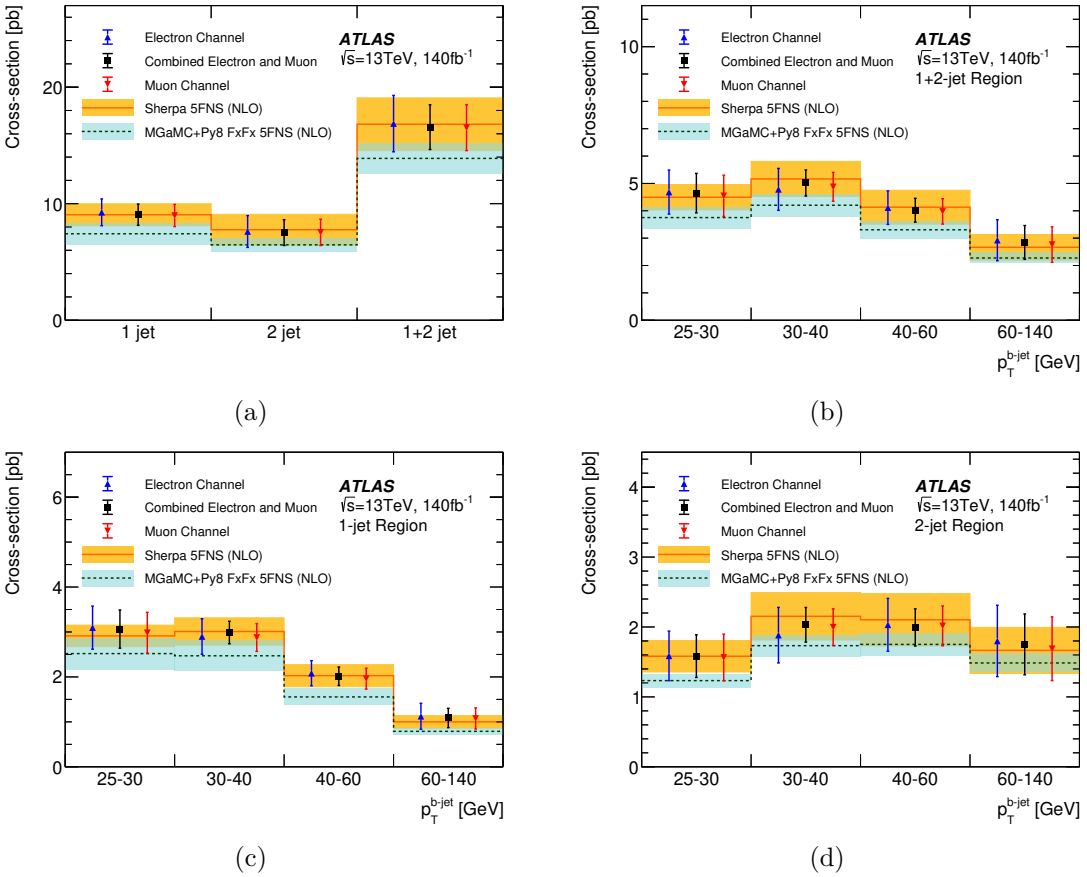


Figure 3. Measured cross-sections and comparisons to theoretical calculations: (a) total fiducial cross-sections, (b) differential cross-sections versus $p_{\mathrm{T}}^{\text{b-jet}}$ in the combined one and two jet region, (c) differential cross-sections versus $p_{\mathrm{T}}^{\text{b-jet}}$ in the one jet region, and (d) differential cross-sections versus $p_{\mathrm{T}}^{\text{b-jet}}$ in the two jet region. The error bars of data points include both statistical and systematic uncertainties, and the error bands of theoretical predictions are from scale and PDF variations.

and 2.0/8 for total cross-sections and differential cross-sections respectively, indicating good consistency between the electron and muon channel results. The statistical uncertainties are treated as uncorrelated between the two channels, while all systematic uncertainties are treated as fully correlated, except for the uncertainties associated with lepton reconstruction, identification, and trigger efficiencies, which are treated as uncorrelated.

The numerical values corresponding to the combination of the electron and muon channels are shown in tables 4 to 7, together with a breakdown of the systematic uncertainties. The total fiducial cross-section measurement has an uncertainty of approximately 10%, dominated by systematic uncertainties, while the statistical uncertainty is about 1%. The systematic uncertainties mainly arise from b-jet performance, with additional sizeable $t\bar{t}$-related contributions in the `2j1b` region due to its higher background fraction. In all regions, the experimental measurements show good agreement with the Sherpa prediction, while the MGaMC+Py8 FxFx results are systematically lower by about one standard deviation. Similarly, for the differential cross-sections, the measurements are dominated by the b-jet

JHEP10(2026)027

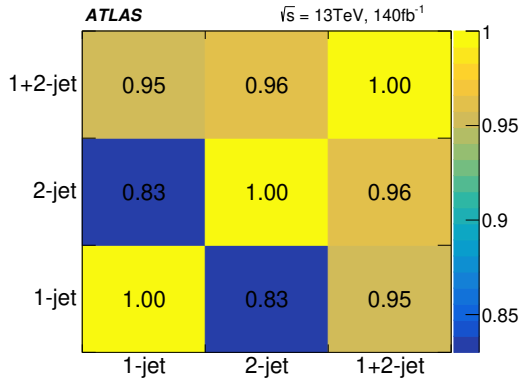


Figure 4. Correlation matrix of the total uncertainties on the total fiducial cross-section.

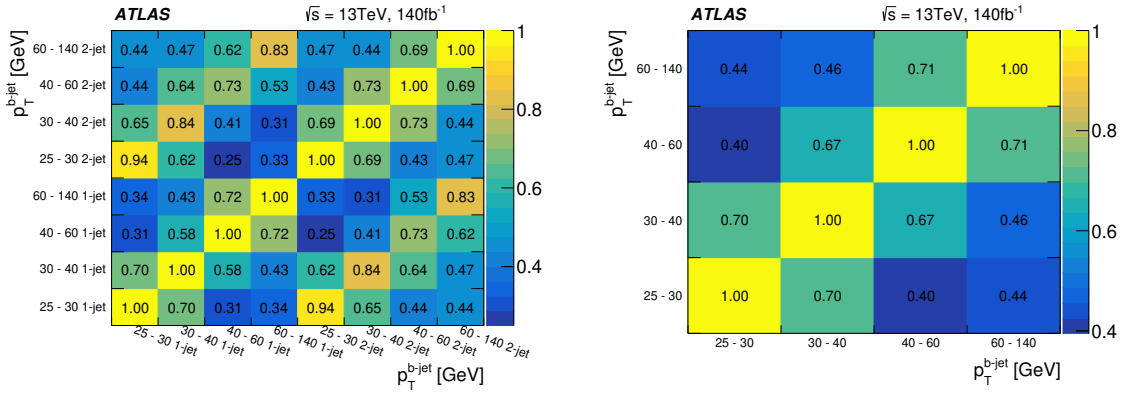


Figure 5. Correlation matrix of the total uncertainties on the combined differential cross-sections in the (a) 1-jet and 2-jet regions where the first four bins are for the 1-jet region and last four bins are for the 2-jet region, and (b) 1+2-jet region.

related systematic uncertainties. However, as the b-jet p_{T} increases, due to the kinematic distribution of the $t\bar{t}$ background, the associated uncertainties increase significantly and gradually become dominant. The measurements in different b-jet p_{T} bins also show good agreement with the Sherpa prediction, while the MGaMC+Py8 FxFx results again exhibit a systematic deficit of about one standard deviation. The correlation matrices for the inclusive and differential measurements are presented in figure 4 and figure 5. As this analysis is dominated by systematic uncertainties and most systematic sources are highly correlated across bins, the correlations are large.

As discussed above, these results correspond to fiducial cross-sections for W boson production in association with one or two b-jets. The cross-sections for W boson production in association with a single b-jet and a non-b-jet can be inferred using the following Sherpa predictions for the fraction of events with one b-jet in the `2j1b` fiducial region: $\{0.98, 0.92, 0.87, 0.84\}$ for the b-jet p_{T} ranges 25–30 GeV, 30–40 GeV, 40–60 GeV, and 60–140 GeV, respectively.

JHEP10(2026)027

Region	1-jet	2-jets	1+2-jets
SHERPA prediction [pb]	9.0 ± 0.9	7.8 ± 1.3	16.8 ± 2.3
MGAMC+PY8 FXFX prediction [pb]	7.4 ± 0.9	6.5 ± 0.6	13.9 ± 1.3
Measured value [pb]	9.1 ± 0.9	7.5 ± 1.1	16.6 ± 1.9
Stat. Unc. [%]	0.8	1.2	0.9
Syst. Unc. [%]	10.1	14.7	11.6
Breakdown of systematic uncertainty [%]			
Stat. Unc. (MC)	0.9	1.2	0.9
V+jet Scale	0.6	1.5	0.8
V+jet PDF	0.6	0.5	0.4
Top background	3.1	7.0	4.3
Electron	1.2	1.7	1.4
Muon	2.2	3.3	2.7
JVT	<0.1	<0.1	<0.1
Jet p_{T}	3.5	3.0	3.1
b-tag	7.3	10.2	8.3
$E_{\mathrm{T}}^{\mathrm{miss}}$	2.6	4.7	3.5
Luminosity	1.3	2.2	1.7
Multijet background	3.3	3.2	3.2
Unfolding	0.4	0.6	<0.1

Table 4. Combined $W + b$-jet fiducial cross-sections with a breakdown of uncertainties. The unfolding uncertainty includes both the statistical uncertainty in the unfolding procedure and the modelling uncertainty. Predictions from both SHERPA and MGAMC+PY8 FXFX are shown for comparison. The uncertainties on the predictions are from scale and PDF variations.

JHEP10(2026)027

$p_{\mathrm{T}}^{\text{b-jet}}$ [GeV]	[25, 30]	[30, 40]	[40, 60]	[60, 140]
Sherpa prediction [pb]	2.91 ± 0.24	3.01 ± 0.30	2.03 ± 0.25	1.00 ± 0.14
MGaMC+Py8 FxFx prediction [pb]	2.52 ± 0.35	2.47 ± 0.34	1.56 ± 0.18	0.79 ± 0.07
Measured value [pb]	3.06 ± 0.43	2.99 ± 0.25	2.01 ± 0.21	1.09 ± 0.21
Stat. Unc. [%]	1.6	1.6	1.8	2.9
Syst. Unc. [%]	13.9	8.4	10.2	19.7
Breakdown of systematic uncertainty [%]				
Stat. Unc. (MC)	2.6	2.0	1.8	2.0
V+jet scale	0.4	0.3	0.7	0.8
V+jet PDF	1.4	0.8	1.1	1.3
Top background	0.8	1.9	4.8	12.9
Electron	1.1	0.6	1.0	3.8
Muon	1.9	1.6	2.3	4.5
JVT	<0.1	<0.1	<0.1	<0.1
Jet p_{T}	2.8	3.0	4.4	7.1
b-tag	12.4	6.3	5.2	6.4
$E_{\mathrm{T}}^{\mathrm{miss}}$	3.1	2.3	3.9	7.7
Luminosity	0.9	1.1	1.7	3.1
Multijet background	1.7	2.1	2.7	5.2
Unfolding	2.4	0.5	1.1	1.0

Table 5. Combined differential cross-sections in the 1-jet region with a breakdown of uncertainties. The unfolding uncertainty includes the statistical uncertainty in the unfolding procedure, the modelling uncertainty and the unfolding bias introduced by the Bayesian unfolding method. Predictions from both Sherpa and MGaMC+Py8 FxFx are shown for comparison. The uncertainties on the predictions are from scale and PDF variations.

JHEP10(2026)027

$p_{\mathrm{T}}^{\text{b-jet}}$ [GeV]	[25, 30]	[30, 40]	[40, 60]	[60, 140]
Sherpa prediction [pb]	1.58 ± 0.23	2.15 ± 0.34	2.10 ± 0.37	1.67 ± 0.33
MGaMC+Py8 FxFx prediction [pb]	1.23 ± 0.10	1.73 ± 0.15	1.75 ± 0.16	1.49 ± 0.13
Measured value [pb]	1.58 ± 0.31	2.03 ± 0.25	1.99 ± 0.27	1.75 ± 0.44
Stat. Unc. [%]	2.2	1.4	1.4	2.5
Syst. Unc. [%]	19.3	12.2	13.3	24.8
Breakdown of systematic uncertainty [%]				
Stat. Unc. (MC)	3.2	1.7	1.4	2.3
V+jet scale	<0.1	0.3	0.5	0.5
V+jet PDF	0.9	0.7	0.6	1.3
Top background	1.6	4.8	7.7	16.0
Electron	1.4	0.9	0.7	2.0
Muon	2.4	1.9	2.7	5.0
JVT	<0.1	<0.1	<0.1	<0.1
Jet p_{T}	4.2	3.2	3.0	7.5
b-tag	17.7	9.7	8.2	11.9
$E_{\mathrm{T}}^{\mathrm{miss}}$	2.9	2.6	4.8	9.7
Luminosity	1.1	1.4	2.1	3.6
Multijet background	1.4	2.0	3.0	5.3
Unfolding	2.9	1.0	0.2	0.8

Table 6. Combined differential cross-sections in the 2-jet region with a breakdown of uncertainties. The unfolding uncertainty includes the statistical uncertainty in the unfolding procedure, the modelling uncertainty and the unfolding bias introduced by the Bayesian unfolding method. Predictions from both Sherpa and MGaMC+Py8 FxFx are shown for comparison. The uncertainties on the predictions are from scale and PDF variations.

JHEP10(2026)027

$p_{\mathrm{T}}^{\text{b-jet}}$ [GeV]	[25, 30]	[30, 40]	[40, 60]	[60, 140]
Sherpa prediction [pb]	4.49 ± 0.46	5.16 ± 0.64	4.13 ± 0.62	2.67 ± 0.47
MGaMC+Py8 FxFx prediction [pb]	3.75 ± 0.39	4.20 ± 0.42	3.31 ± 0.32	2.27 ± 0.20
Measured value [pb]	4.64 ± 0.72	5.02 ± 0.48	4.02 ± 0.44	2.84 ± 0.62
Stat. Unc. [%]	1.6	1.4	1.3	1.9
Syst. Unc. [%]	15.6	9.5	10.9	21.7
Breakdown of systematic uncertainty [%]				
Stat. Unc. (MC)	2.6	1.7	1.3	1.8
V+jet Scale	0.4	0.4	0.5	0.6
V+jet PDF	1.3	0.7	0.4	1.1
Top background	0.9	3.0	5.8	13.8
Electron	1.2	0.5	0.7	2.1
Muon	2.1	1.7	2.4	4.7
JVT	<0.1	<0.1	<0.1	<0.1
Jet p_{T}	2.9	2.7	3.3	7.0
b-tag	14.2	7.6	6.2	9.6
$E_{\mathrm{T}}^{\mathrm{miss}}$	3.0	2.3	4.4	8.8
Luminosity	0.9	1.2	1.9	3.4
Multijet background	1.6	2.0	2.7	5.3
Unfolding	2.6	0.7	0.6	0.9

Table 7. Combined differential cross-sections in the 1+2-jet region with a breakdown of uncertainties. The unfolding uncertainty includes the statistical uncertainty in the unfolding procedure, the modelling uncertainty and the unfolding bias introduced by the Bayesian unfolding method. Predictions from both Sherpa and MGaMC+Py8 FxFx are shown for comparison. The uncertainties on the predictions are from scale and PDF variations.

JHEP10(2026)027

9 Conclusions

A measurement of the cross-section of W boson production in association with b-jets at $\sqrt{s} = 13\,\text{TeV}$ is presented, based on data corresponding to an integrated luminosity of 140 fb^{-1} collected with the ATLAS detector at the LHC in Run 2. The analysis defines two signal regions with exactly one or two jets in the final state, requiring exactly one of the jets to be b-tagged. The signal yields are estimated separately in the electron and muon decay channels and unfolded to a common fiducial phase space. Good agreement is observed between the results in the electron and muon channels, and combined measurements are provided.

The measured fiducial cross-sections in the 1-jet, 2-jets and 1+2 jets combined regions are:

$$\begin{aligned}
\sigma_{\text{fid}}(\text{1-jet}) &= 9.1 \pm 0.1\ (\text{stat.}) \ \pm 0.9\ (\text{syst.})\ \text{pb},\\
\sigma_{\text{fid}}(\text{2-jets}) &= 7.5 \pm 0.1\ (\text{stat.}) \ \pm 1.1\ (\text{syst.})\ \text{pb},\\
\sigma_{\text{fid}}(\text{1+2 jets}) &= 16.6 \pm 0.2\ (\text{stat.}) \ \pm 1.9\ (\text{syst.})\ \text{pb}.
\end{aligned}$$

They are found to be consistent with the Sherpa predictions, while being larger than the MGaMC+Py8 FxFx predictions by approximately one standard deviation. The uncertainty on the total cross-section is about 10% and is dominated by systematic uncertainties. The precision of theory predictions is limited by missing higher-order uncertainties, which are estimated through scale variations to be approximately at the 10% level.

A differential cross-section measurement as a function of the leading b-jet p_{T} is also presented, for jets with p_{T} in the range of 25 GeV to 140 GeV. The measured differential cross-sections show good agreement with the theoretical predictions.

Compared to the previous ATLAS 7 TeV measurement [8], the statistical uncertainty is reduced approximately by a factor of ten and the systematic uncertainty by a factor of two. This improvement is primarily due to the much larger dataset and improved jet and b-tagging performance.

Acknowledgments

We thank CERN for the very successful operation of the LHC and its injectors, as well as the support staff at CERN and at our institutions worldwide without whom ATLAS could not be operated efficiently.

The crucial computing support from all WLCG partners is acknowledged gratefully, in particular from CERN, the ATLAS Tier-1 facilities at TRIUMF/SFU (Canada), NDGF (Denmark, Norway, Sweden), CC-IN2P3 (France), KIT/GridKA (Germany), INFN-CNAF (Italy), NL-T1 (Netherlands), PIC (Spain), RAL (U.K.) and BNL (U.S.A.), the Tier-2 facilities worldwide and large non-WLCG resource providers. Major contributors of computing resources are listed in ref. [55].

We gratefully acknowledge the support of ANPCyT, Argentina; YerPhI, Armenia; ARC, Australia; BMWFW and FWF, Austria; ANAS, Azerbaijan; CNPq and FAPESP, Brazil; NSERC, NRC and CFI, Canada; CERN; ANID, Chile; CAS, MOST, NSFC and FRFCU, China; Minciencias, Colombia; MEYS CR, Czech Republic; DNRF and DNSRC, Denmark; IN2P3-CNRS and CEA-DRF/IRFU, France; SRNSFG, Georgia; BMFTR, HGF and MPG,

JHEP10(2026)027

Germany; GSRI, Greece; RGC and Hong Kong SAR, China; ICHEP and Academy of Sciences and Humanities, Israel; INFN, Italy; MEXT and JSPS, Japan; CNRST, Morocco; NWO, Netherlands; RCN, Norway; MNiSW, Poland; FCT, Portugal; MNE/IFA, Romania; MSTDI, Serbia; MSSR, Slovakia; ARIS and MVZI, Slovenia; DSI/NRF, South Africa; MICIU/AEI, Spain; SRC and Wallenberg Foundation, Sweden; SERI, SNSF and Cantons of Bern and Geneva, Switzerland; NSTC, Taipei; TENMAK, Türkiye; STFC/UKRI, United Kingdom; DOE and NSF, United States of America.

Individual groups and members have received support from BCKDF, CANARIE, CRC and DRAC, Canada; CERN-CZ, FORTE and PRIMUS, Czech Republic; COST, ERC, ERDF, Horizon 2020 and Marie Skłodowska-Curie Actions, European Union; Investissements d'Avenir Labex, Investissements d'Avenir Idex and ANR, France; DFG and AvH Foundation, Germany; Herakleitos, Thales and Aristeia programmes co-financed by EU-ESF and the Greek NSRF, Greece; BSF-NSF and MINERVA, Israel; NCN and NAWA, Poland; La Caixa Banking Foundation, CERCA and AGAUR programs from Generalitat de Catalunya and PROMETEO and GenT Programmes Generalitat Valenciana, Spain; Göran Gustafssons Stiftelse, Sweden; The Royal Society and Leverhulme Trust, United Kingdom; Eric and Wendy Schmidt Fund for Strategic Innovation, United States of America.

In addition, individual members wish to acknowledge support from Chile: Agencia Nacional de Investigación y Desarrollo (ANID FONDECYT reg. 1230987, FONDECYT 1230812, FONDECYT 1240864, Fondecyt 3240661, Fondecyt Regular 1240721); China: Fundamental Research Funds for the Central Universities (010-63263105), Chinese Ministry of Science and Technology (MOST-2023YFA1605700, MOST-2023YFA1609300), National Natural Science Foundation of China (NSFC 12275265, NSFC-W2543005); Czech Republic: Czech Science Foundation (GACR — 24-11373S), Ministry of Education Youth and Sports (ERC-CZ-LL2327, FORTE CZ.02.01.01/00/22_008/0004632); EU: H2020 European Research Council (ERC — 101002463); European Union: European Research Council (BARD No. 101116429, ERC — 101219398, ERC 101089007), European Regional Development Fund (HE COFUND GA No.101081355, ERDF), Marie Sklodowska-Curie Actions (GAP-101168829); France: Agence Nationale de la Recherche (ANR-21-CE31-0013, ANR-22-EDIR-0002, ANR-24-CE31-0504-01); Germany: Deutsche Forschungsgemeinschaft (DFG — 469666862); China: Research Grants Council (GRF); Italy: Istituto Nazionale di Fisica Nucleare (LHC-MIUR — 28003/2025), Ministero dell'Università e della Ricerca (NextGenEU I53D23000820006 M4C2.1.1, SOE2024_0000023); Japan: Japan Society for the Promotion of Science (JSPS KAKENHI JP25H0063, JSPS KAKENHI JP22H04944, JSPS KAKENHI JP24K23939, JSPS KAKENHI JP24KK0251, JSPS KAKENHI JP25H00650, JSPS KAKENHI JP25H01291, JSPS KAKENHI JP25K01011, JSPS KAKENHI JP25K01023, JSPS KAKENHI JP25KK0047); Poland: Polish National Science Centre (NCN 2021/42/E/ST2/00350, NCN OPUS 2023/51/B/ST2/02507, NCN OPUS nr 2022/47/B/ST2/03059, NCN UMO-2019/34/E/ST2/00393, UMO-2022/47/O/ST2/00148, UMO-2023/49/B/ST2/04085, UMO-2023/51/B/ST2/00920, UMO-2024/53/N/ST2/00869); Spain: Agència de Gestió d'Ajuts Universitaris i de Recerca. (AGAUR — 2023 BP 00141), Ministry of Science and Innovation (RYC2019-028510-I, RYC2020-030254-I, RYC2021-031273-I, RYC2022-038164-I), Ministerio de Ciencia, Innovación y Universidades/Agencia Estatal de Investigación

(EU NextGenerationEU (PRTR-C17.I1), PID2022-142604OB-C22); Sweden: Carl Trygger Foundation (Carl Trygger Foundation CTS 22:2312), Swedish Research Council (Swedish Research Council 2023-04654, VR 2021-03651, VR 2022-03845, VR 2022-04683, VR 2023-03403, VR 2024-05451, VR 2025-05940), Knut and Alice Wallenberg Foundation (KAW 2023.0366); United Kingdom: The Binks Trust, Royal Society (NIF-R1-231091); United States of America: U.S. Department of Energy (ECA DE-AC02-76SF00515), John Templeton Foundation (John Templeton Foundation 63206), Neubauer Family Foundation.

Data Availability Statement. The public release of data supporting the findings of this article will follow the CERN Open Data Policy [56]. Inquiries about plots and tables associated with this article can be addressed to atlas.publications@cern.ch.

Code Availability Statement. The ATLAS collaboration's Athena software, including the configuration of the event generators, is open source (`http://gitlab.cern.ch/atlas/athena`).

Open Access. This article is distributed under the terms of the Creative Commons Attribution License (CC-BY4.0), which permits any use, distribution and reproduction in any medium, provided the original author(s) and source are credited.

References

[1] J.M. Campbell et al., *NLO QCD predictions for $W+1$ jet and $W+2$ jet production with at least one b jet at the 7 TeV LHC*, *Phys. Rev. D* **86** (2012) 034021 [arXiv:1107.3714] [INSPIRE].

[2] J.M. Campbell et al., *Associated production of a W boson and one b jet*, *Phys. Rev. D* **79** (2009) 034023 [arXiv:0809.3003] [INSPIRE].

[3] ATLAS collaboration, *Measurements of WH and ZH production with Higgs boson decays into bottom quarks and direct constraints on the charm Yukawa coupling in 13 TeV pp collisions with the ATLAS detector*, *JHEP* **04** (2025) 075 [arXiv:2410.19611] [INSPIRE].

[4] ATLAS collaboration, *Search for heavy neutral leptons in decays of W bosons using leptonic and semi-leptonic displaced vertices in $\sqrt{s} = 13$ TeV pp collisions with the ATLAS detector*, *JHEP* **07** (2025) 196 [arXiv:2503.16213] [INSPIRE].

[5] ATLAS collaboration, *Measurement of single top-quark production in the s-channel in proton–proton collisions at $\sqrt{s} = 13$ TeV with the ATLAS detector*, *JHEP* **06** (2023) 191 [arXiv:2209.08990] [INSPIRE].

[6] CDF collaboration, *First measurement of the b-jet cross section in events with a W boson in $p\bar{p}$ collisions at $\sqrt{s} = 1.96$ TeV*, *Phys. Rev. Lett.* **104** (2010) 131801 [arXiv:0909.1505] [INSPIRE].

[7] D0 collaboration, *Measurement of the $W+b$-jet and $W+c$-jet differential production cross sections in $p\bar{p}$ collisions at $\sqrt{s} = 1.96$ TeV*, *Phys. Lett. B* **743** (2015) 6 [arXiv:1412.5315] [INSPIRE].

[8] ATLAS collaboration, *Measurement of the cross-section for W boson production in association with b-jets in pp collisions at $\sqrt{s} = 7$ TeV with the ATLAS detector*, *JHEP* **06** (2013) 084 [arXiv:1302.2929] [INSPIRE].

[9] CMS collaboration, *Measurement of the production cross section for a W boson and two b jets in pp collisions at $\sqrt{s} = 7$ TeV*, *Phys. Lett. B* **735** (2014) 204 [arXiv:1312.6608] [INSPIRE].

JHEP10(2026)027

[10] CMS collaboration, *Measurement of the production cross section of a W boson in association with two b jets in pp collisions at $\sqrt{s} = 8$ TeV*, *Eur. Phys. J. C* **77** (2017) 92 [arXiv:1608.07561] [INSPIRE].

[11] ATLAS collaboration, *Luminosity determination in pp collisions at $\sqrt{s} = 13$ TeV using the ATLAS detector at the LHC*, *Eur. Phys. J. C* **83** (2023) 982 [arXiv:2212.09379] [INSPIRE].

[12] ATLAS collaboration, *The ATLAS experiment at the CERN Large Hadron Collider*, 2008 *JINST* **3** S08003 [INSPIRE].

[13] G. Avoni et al., *The new LUCID-2 detector for luminosity measurement and monitoring in ATLAS*, 2018 *JINST* **13** P07017 [INSPIRE].

[14] ATLAS collaboration, *Performance of the ATLAS trigger system in 2015*, *Eur. Phys. J. C* **77** (2017) 317 [arXiv:1611.09661] [INSPIRE].

[15] ATLAS collaboration, *Performance of electron and photon triggers in ATLAS during LHC run 2*, *Eur. Phys. J. C* **80** (2020) 47 [arXiv:1909.00761] [INSPIRE].

[16] ATLAS collaboration, *Performance of the ATLAS muon triggers in run 2*, 2020 *JINST* **15** P09015 [arXiv:2004.13447] [INSPIRE].

[17] SHERPA collaboration, *Event generation with Sherpa 2.2*, *SciPost Phys.* **7** (2019) 034 [arXiv:1905.09127] [INSPIRE].

[18] ATLAS collaboration, *Modelling and computational improvements to the simulation of single vector-boson plus jet processes for the ATLAS experiment*, *JHEP* **08** (2022) 089 [arXiv:2112.09588] [INSPIRE].

[19] NNPDF collaboration, *Parton distributions for the LHC run II*, *JHEP* **04** (2015) 040 [arXiv:1410.8849] [INSPIRE].

[20] J. Alwall et al., *The automated computation of tree-level and next-to-leading order differential cross sections, and their matching to parton shower simulations*, *JHEP* **07** (2014) 079 [arXiv:1405.0301] [INSPIRE].

[21] R. Frederix and S. Frixione, *Merging meets matching in MC@NLO*, *JHEP* **12** (2012) 061 [arXiv:1209.6215] [INSPIRE].

[22] T. Sjöstrand et al., *An introduction to PYTHIA 8.2*, *Comput. Phys. Commun.* **191** (2015) 159 [arXiv:1410.3012] [INSPIRE].

[23] ATLAS collaboration, *ATLAS Pythia 8 tunes to 7 TeV data*, ATL-PHYS-PUB-2014-021 (2014) [INSPIRE].

[24] NNPDF collaboration, *Illuminating the photon content of the proton within a global PDF analysis*, *SciPost Phys.* **5** (2018) 008 [arXiv:1712.07053] [INSPIRE].

[25] S. Frixione, P. Nason and G. Ridolfi, *A positive-weight next-to-leading-order Monte Carlo for heavy flavour hadroproduction*, *JHEP* **09** (2007) 126 [arXiv:0707.3088] [INSPIRE].

[26] P. Nason, *A new method for combining NLO QCD with shower Monte Carlo algorithms*, *JHEP* **11** (2004) 040 [hep-ph/0409146] [INSPIRE].

[27] S. Frixione, P. Nason and C. Oleari, *Matching NLO QCD computations with parton shower simulations: the POWHEG method*, *JHEP* **11** (2007) 070 [arXiv:0709.2092] [INSPIRE].

[28] S. Alioli, P. Nason, C. Oleari and E. Re, *A general framework for implementing NLO calculations in shower Monte Carlo programs: the POWHEG BOX*, *JHEP* **06** (2010) 043 [arXiv:1002.2581] [INSPIRE].

JHEP10(2026)027

[29] M. Czakon et al., *Top-pair production at the LHC through NNLO QCD and NLO EW*, *JHEP* **10** (2017) 186 [arXiv:1705.04105] [INSPIRE].

[30] ATLAS collaboration, *The ATLAS simulation infrastructure*, *Eur. Phys. J. C* **70** (2010) 823 [arXiv:1005.4568] [INSPIRE].

[31] GEANT4 collaboration, *GEANT4 — a simulation toolkit*, *Nucl. Instrum. Meth. A* **506** (2003) 250 [INSPIRE].

[32] ATLAS collaboration, *The Pythia 8 A3 tune description of ATLAS minimum bias and inelastic measurements incorporating the Donnachie-Landshoff diffractive model*, ATL-PHYS-PUB-2016-017 (2016) [INSPIRE].

[33] R.D. Ball et al., *Parton distributions with LHC data*, *Nucl. Phys. B* **867** (2013) 244 [arXiv:1207.1303] [INSPIRE].

[34] ATLAS collaboration, *Electron reconstruction and identification in the ATLAS experiment using the 2015 and 2016 LHC proton-proton collision data at* $\sqrt{s} = 13$ *TeV*, *Eur. Phys. J. C* **79** (2019) 639 [arXiv:1902.04655] [INSPIRE].

[35] ATLAS collaboration, *Electron and photon efficiencies in LHC run 2 with the ATLAS experiment*, *JHEP* **05** (2024) 162 [arXiv:2308.13362] [INSPIRE].

[36] ATLAS collaboration, *Muon reconstruction and identification efficiency in ATLAS using the full Run 2 pp collision data set at* $\sqrt{s} = 13$ *TeV*, *Eur. Phys. J. C* **81** (2021) 578 [arXiv:2012.00578] [INSPIRE].

[37] ATLAS collaboration, *The performance of missing transverse momentum reconstruction and its significance with the ATLAS detector using* $140\,fb^{-1}$ *of* $\sqrt{s} = 13$ *TeV pp collisions*, *Eur. Phys. J. C* **85** (2025) 606 [arXiv:2402.05858] [INSPIRE].

[38] M. Cacciari, G.P. Salam and G. Soyez, *The anti-*k_t *jet clustering algorithm*, *JHEP* **04** (2008) 063 [arXiv:0802.1189] [INSPIRE].

[39] M. Cacciari, G.P. Salam and G. Soyez, *FastJet user manual*, *Eur. Phys. J. C* **72** (2012) 1896 [arXiv:1111.6097] [INSPIRE].

[40] ATLAS collaboration, *Jet reconstruction and performance using particle flow with the ATLAS detector*, *Eur. Phys. J. C* **77** (2017) 466 [arXiv:1703.10485] [INSPIRE].

[41] ATLAS collaboration, *Jet energy scale measurements and their systematic uncertainties in proton-proton collisions at* $\sqrt{s} = 13$ *TeV with the ATLAS detector*, *Phys. Rev. D* **96** (2017) 072002 [arXiv:1703.09665] [INSPIRE].

[42] ATLAS collaboration, *Tagging and suppression of pileup jets*, ATLAS-CONF-2014-018 (2014) [INSPIRE].

[43] ATLAS collaboration, *ATLAS flavour-tagging algorithms for the LHC run 2 pp collision dataset*, *Eur. Phys. J. C* **83** (2023) 681 [arXiv:2211.16345] [INSPIRE].

[44] ATLAS collaboration, *Measurements of the production cross-section for a Z boson in association with b- or c-jets in proton–proton collisions at* $\sqrt{s} = 13$ *TeV with the ATLAS detector*, *Eur. Phys. J. C* **84** (2024) 984 [arXiv:2403.15093] [INSPIRE].

[45] ATLAS collaboration, *Tools for estimating fake/non-prompt lepton backgrounds with the ATLAS detector at the LHC*, 2023 *JINST* **18** T11004 [arXiv:2211.16178] [INSPIRE].

[46] ATLAS collaboration, *ATLAS b-jet identification performance and efficiency measurement with* $t\bar{t}$ *events in pp collisions at* $\sqrt{s} = 13$ *TeV*, *Eur. Phys. J. C* **79** (2019) 970 [arXiv:1907.05120] [INSPIRE].

JHEP10(2026)027

[47] ATLAS collaboration, *Calibration of the light-flavour jet mistagging efficiency of the b-tagging algorithms with Z+jets events using 139 fb^{-1} of ATLAS proton–proton collision data at $\sqrt{s} = 13$ TeV*, *Eur. Phys. J. C* **83** (2023) 728 [arXiv:2301.06319] [INSPIRE].

[48] ATLAS collaboration, *Measurement of the c-jet mistagging efficiency in $t\bar{t}$ events using pp collision data at $\sqrt{s} = 13$ TeV collected with the ATLAS detector*, *Eur. Phys. J. C* **82** (2022) 95 [arXiv:2109.10627] [INSPIRE].

[49] ATLAS collaboration, *Evaluating statistical uncertainties and correlations using the bootstrap method*, ATL-PHYS-PUB-2021-011 (2021) [INSPIRE].

[50] G. D'Agostini, *A multidimensional unfolding method based on Bayes' theorem*, *Nucl. Instrum. Meth. A* **362** (1995) 487 [INSPIRE].

[51] ATLAS collaboration, *Simulation-based extrapolation of b-tagging calibrations towards high transverse momenta in the ATLAS experiment*, ATL-PHYS-PUB-2021-003 (2021) [INSPIRE].

[52] ATLAS collaboration, *Inclusive and differential cross-sections for dilepton $t\bar{t}$ production measured in $\sqrt{s} = 13$ TeV pp collisions with the ATLAS detector*, *JHEP* **07** (2023) 141 [arXiv:2303.15340] [INSPIRE].

[53] L. Lyons, D. Gibaut and P. Clifford, *How to combine correlated estimates of a single physical quantity*, *Nucl. Instrum. Meth. A* **270** (1988) 110 [INSPIRE].

[54] A. Pinto et al., *Uncertainty components in profile likelihood fits*, *Eur. Phys. J. C* **84** (2024) 593 [arXiv:2307.04007] [INSPIRE].

[55] ATLAS collaboration, *ATLAS computing acknowledgements*, ATL-SOFT-PUB-2026-001, CERN, Geneva, Switzerland (2026).

[56] *CERN Open Data Policy for the LHC experiments*, CERN-OPEN-2020-013, CERN, Geneva, Switzerland (2020).

JHEP10(2026)027

The ATLAS collaboration

G. Aad[102], E. Aakvaag[17], B. Abbott[121], S. Abdelhameed[83b], K. Abeling[54], N.J. Abicht[48], S.H. Abidi[30], M. Aboelela[44], A. Aboulhorma[36e], H. Abramowicz[154], B.S. Acharya[68a,68b,a], A. Ackermann[62a], J. Ackerschott[55], C. Adam Bourdarios[4], L. Adamczyk[85a], S.V. Addepalli[146], M. J. Addison[101], J. Adelman[117], A. Adiguzel[22c], T. Adye[135], A.A. Affolder[137], Y. Afik[39], M.N. Agaras[13], A. Aggarwal[100], C. Agheorghiesei[28c], A. Ahmad[83a], F. Ahmadov[38,b], S. Ahuja[165], X. Ai[113c], G. Aielli[75a,75b], A. Aikot[165], M. Ait Tamlihat[36e], T.P.A. Åkesson[98], D. Akiyama[170], N.N. Akolkar[25], S. Aktas[168], G.L. Alberghi[24b], J. Albert[167], U. Alberti[20], P. Albicocco[52], S. Alderweireldt[51], Z.L. Alegria[122], M. Aleksa[37], I.N. Aleksandrov[38], C. Alexa[28b], T. Alexopoulos[10], F. Alfonsi[24b], M. Algren[55], M. Alhroob[169], B. Ali[133], H. M. J. Ali[91,c], S. Ali[32], S.W. Alibocus[92], M. Aliev[34c], G. Alimonti[70a], C. Allaire[65], B.M.M. Allbrooke[149], D. R. Allen[122], J. S. Allen[101], J.F. Allen[51], C.S. Alley[1], E.R. Almazan[137], A. Aloisio[71a,71b], F. Alonso[90], C. Alpigiani[140], A. Alvarez Fernandez[100], M. Alves Cardoso[55], M.G. Alviggi[71a,71b], Y. Amaral Coutinho[81b], C. Amelung[37], M. Amerl[101], T. Amezza[128], B. Amini[53], K. Amirie[158], A. Amirkhanov[38], D. Amperiadou[155], C. Anastopoulos[142], T. Andeen[11], J.K. Anders[92], A. C. Anderson[58], A. Andreazza[70a,70b], S. Angelidakis[9], A. Angerami[41], A.V. Anisenkov[38], A. Annovi[73a], C. Antel[37], E. Antipov[148], M. Antonelli[52], F. Anulli[74a], M. Aoki[82], T. Aoki[156], M.A. Aparo[13], L. Aperio Bella[47], M. Apicella[31], C. Appelt[154], A. Apyan[27], R. Arakida[125], M. Arampatzi[10], S. J. Arbiol Val[86], C. Arcangeletti[52], A.T.H. Arce[50], M. Arcuri[43b,43a], J-F. Arguin[108], S. Argyropoulos[155], J.-H. Arling[47], O. Arnaez[4], A.P. Arnold[94], H. Arnold[148], G. Artoni[74a,74b], H. Asada[111], S. Asatryan[175], N.A. Asbah[37], R. A. Ashby Pickering[169], A. M. Aslam[95], J. Assahsah[36d], K. Assamagan[30], R. Astalos[29a], K. S. V. Astrand[98], S. Atashi[162], R.J. Atkin[34a], H. Atmani[36f], P.A. Atmasiddha[129], K. Augsten[133], A.D. Auriol[40], V.A. Austrup[101], A.S. Avad[94], G. Avolio[37], A. Azzam[13], D. Babal[29b], H. Bachacou[136], K. Bachas[155,d], A. Bachiu[35], E. Bachmann[49], M. J. Backes[62a], A. Badea[39], T.M. Baer[106], M. Bahmani[19], D. Bahner[53], K. Bai[124], L. Baines[94], O.K. Baker[174], D. Bakshi Gupta[8], L.E. Balabram Filho[81b], V. Balakrishnan[121], R. Balasubramanian[4], P. Balek[85a], E. Ballabene[24b,24a], F. Balli[136], L.M. Baltes[62a], W.K. Balunas[127], I. Bamwidhi[83c], E. Banas[86], M. Bandieramonte[130], S. Bansal[25], L. Barak[154], M. Barakat[47], E.L. Barberio[105], D. Barberis[18b], M. Barbero[102], M. Z. Barel[116], T. Barillari[110], M-S. Barisits[37], T. Barklow[146], P. Baron[134], D.A. Baron Moreno[101], A. Baroncelli[61], A.J. Barr[127,e], J.D. Barr[96], F. Barreiro[99], J. Barreiro Guimarães da Costa[14], M.G. Barros Teixeira[131a], F. Bartels[37], R. Bartoldus[146], A.E. Barton[91], P. Bartos[29a], M. Baselga[48], S. Bashiri[86], A. Bassalat[65,f], M.J. Basso[159a], S. Bataju[44], R. Bate[166], R.L. Bates[58], M. Battaglia[137], D. Battulga[19], M. Bauce[74a,74b], L. Bauckhage[47], P. Bauer[25], L. T. Bayer[47], L.T. Bazzano Hurrell[31], T. Beau[128], J.Y. Beaucamp[90], S. Beauceron[128], P.H. Beauchemin[161], P. Bechtle[25], H.P. Beck[20,g], K. Becker[169], A.J. Beddall[80], V.A. Bednyakov[38], C.P. Bee[148], L.J. Beemster[16], M. Begalli[81d], M. Begel[30], J.K. Behr[47], J.F. Beirer[37], F. Beisiegel[25], I.B. Belean[28d], M. Belfkir[83c], G. Bella[154], L. Bellagamba[24b], A. Bellerive[35], C.D. Bellgraph[67], P. Bellos[21], I. Benaoumeur[21], D. Benchekroun[36a], F. Bendebba[36a], Y. Benhammou[154],

JHEP10(2026)027

K.C. Benkendorfer[167], L. Beresford[47], M. Beretta[52], E. Bergeaas Kuutmann[163], N. Berger[4], B. Bergmann[133], J. Beringer[18a], M. Berkat[136], G. Bernardi[5], C. Bernius[146], F.U. Bernlochner[25], A. Berrocal Guardia[13], T. Berry[95], P. Berta[134], A. Berti[131a], R. Bertrand[102], S. Bethke[110], A. Betti[74a,74b], T.F. Beumker[173], A.J. Bevan[94], L. Bezio[55], N.K. Bhalla[53], S. Bharthuar[110], S. Bhatta[148], P. Bhattarai[146], Z.M. Bhatti[118], K. D. Bhide[164], V.S. Bhopatkar[122], R.M. Bianchi[130], G. Bianco[24b,24a], O. Biebel[109], M. Biglietti[76a], P. Bijl[53], C. S. Billingsley[44], Y. Bimgdi[36f], M. Bindi[54], A. Bingham[173], A. Bingul[22b], C. Bini[74a,74b], M. Biros[134], S. Biryukov[149], T. Bisanz[48], E. Bisceglie[24b,24a], J.P. Biswal[135], D. Biswas[144], M. Biyabi[14], I. Bloch[47], A. Blue[58], U. Blumenschein[94], V.S. Bobrovnikov[38], L. Boccardo[56b,56a], M. Boehler[53], D. Bogavac[13], L. S. Boggia[128], V. Boisvert[95], P. Bokan[163], T. Bold[85a], M. Bomben[5], M. Bona[94], M. Boonekamp[136], A.G. Borbély[58], G. Borissov[91], A. Borkar[168], D. Bortoletto[127], M. Borysova[171], D. Boscherini[24b], M. Bosman[13], K. Bouaouda[36a], L. Boudet[136], J. Boudreau[130], E.V. Bouhova-Thacker[91], D. Boumediene[40], R. Bouquet[56b,56a], A. Boveia[120], D. Boye[30], I.R. Boyko[38], L. Bozianu[55], J. Bracinik[21], N. Brahimi[4], G. Brandt[173], O. Brandt[33], B. Brau[103], R. Brener[171], L. Brenner[116], R. Brenner[163], S. Bressler[171], M. Brettell[96], G. Brianti[116], D. Britton[58], D. Britzger[110], I. Brock[25], R. Brock[107], H. Bronson[129], G. Brooijmans[41], A.J. Brooks[67], E. M. Brooks[159b], E. Brost[30], L.M. Brown[167,159a], L.E. Bruce[60], T.L. Bruckler[127], P.A. Bruckman de Renstrom[86], B. Brüers[47], A. Bruni[24b], G. Bruni[24b], D. Brunner[46a,46b], M. Bruschi[24b], N. Bruscino[74a,74b], T. Buanes[17], Q. Buat[140], D. Buchin[110], A.G. Buckley[58], J. Bucko[134], M. Buhring[49], O. Bulekov[80], B.A. Bullard[146], T. O. Buratovich[90], S. Burdin[92], C.D. Burgard[48], A.M. Burger[89], B. Burghgrave[8], O. Burlayenko[53], J. Burleson[164], J.C. Burzynski[121], V. Büscher[100], P.J. Bussey[58], O. But[25], J.M. Butler[26], C.M. Buttar[58], J.M. Butterworth[96], P. Butti[37], W. Buttinger[135], C.J. Buxo Vazquez[107], A.R. Buzykaev[38], S. Cabrera Urbán[165], L. Cadamuro[65], H. Cai[37], Y. Cai[24b,112c,24a], Y. Cai[112a], M.A. Cairo[129], V.M.M. Cairo[37], O. Cakir[3a], N. Calace[37], P. Calafiura[18a], G. Calderini[128], P. Calfayan[35], L. Calic[98], G. Callea[58], L.P. Caloba[81b], D. Calvet[40], S. Calvet[40], R. Camacho Toro[128], S. Camarda[37], D. Camarero Munoz[27], P. Camarri[75a,75b], C. Camincher[37], M. Campanelli[96], A. Camplani[42], V. Canale[71a,71b], A.C. Canbay[3a], E. Canonero[95], J. Cantero[165], F. Capocasa[27], P. Cappelli[27], M. Capua[43b,43a], A. Carbone[70a,70b], R. Cardarelli[75a], J.C.J. Cardenas[8], M. P. Cardiff[27], G. Carducci[43b,43a], T. Carli[37], G. Carlino[71a], J.I. Carlotto[13], B.T. Carlson[130,h], E.M. Carlson[167], L. Carminati[70a,70b], A. Carnelli[4], M. Carnesale[37], S. Caron[115], E. Carquin[138g], I.B. Carr[105], S. Carrà[72a,72b], G. Carratta[24b,24a], C. Carrion Martinez[165], A.M. Carroll[124], N. Cartalade[40], M.P. Casado[13,i], A. Casali[58], P. Casolaro[71a,71b], M. Caspar[47], F. Cassinese[90], F. Castiglioni[73a,73b], W.R. Castiglioni[39], F.L. Castillo[4], V. Castillo Gimenez[165], N.F. Castro[131a,131e], A. Catinaccio[37], J.R. Catmore[126], T. Cavaliere[4], V. Cavaliere[30], E. Celebi[80], S. Cella[30], V. Cepaitis[55], K. Cerny[123], A.S. Cerqueira[81a], A. Cerri[73a,j], L. Cerrito[75a,75b], F. Cerutti[18a], B. Cervato[70a,70b], A. Cervelli[24b], G. Cesarini[52], S.A. Cetin[80], V. C. Chabalala[34j], P.M. Chabrillat[128], R. Chakkappai[65], S. Chakraborty[169], A. Chambers[60], J. Chan[18a], J.D. Chapman[33], E. Chapon[136], D.G. Charlton[21], C. Chauhan[132], Y. Che[112a], S. Chekanov[6], G.A. Chelkov[38,k], H. Chen[30], J. Chen[141a],

JHEP10(2026)027

J. Chen[145], M. Chen[59], S. Chen[87], S.J. Chen[112a], X. Chen[141a], X. Chen[15,l], Z. Chen[61], C.L. Cheng[146], H.C. Cheng[63a], S. Cheong[146], A. Cheplakov[38], E. Cherepanova[116], E. Cheu[7], K. Cheung[64], L. Chevalier[136], G. Chiarelli[73a], G. Chiodini[69a], A.S. Chisholm[21], J. L. Chisholm[166], A. Chitan[28b], M. Chitishvili[165], M.V. Chizhov[38,m], K. Chmiel[76a,76b], K. Choi[11], Y. Chou[140], E.Y.S. Chow[115], G. Christou[51], K.L. Chu[171], M.C. Chu[63a], Z. Chubinidze[52], J. Chudoba[132], J.J. Chwastowski[86], D. Cieri[110], K.M. Ciesla[85a], V. Cindro[93], A. Ciocio[18a], F. Cirotto[71a,71b], Z.H. Citron[171], M. Citterio[70a], D.A. Ciubotaru[28b], A. Clark[55], P.J. Clark[51], N. Clarke Hall[37], C. Clarry[158], S.E. Clawson[37], C. Clement[46a,46b], L. Clissa[24b,24a], Y. Coadou[102], M. Cobal[68a,68c], A. Coccaro[56b], M. G. Cochran Branson[140], R.F. Coelho Barrue[131a], R. Coelho Lopes De Sa[103], S. Coelli[70a], M.M. Cohen[129], L. S. Colangeli[158], B. Cole[41], P. Collado Soto[99], J. Collot[59], M.R. Coluccia[69a], I. Combes[65], P. Conde Muiño[131a,131g], L.H.J. Condren[162], M.P. Connell[34c], S.H. Connell[34c], E.I. Conroy[161], M. Contreras Cossio[11], F. Conventi[71a,n], A.M. Cooper-Sarkar[127], L. Corazzina[74a,74b], F. A. Corchia[24b,24a], A. Cordeiro Oudot Choi[140], L.D. Corpe[40], M. Corradi[74a,74b], F. Corriveau[104,o], A. Cortes-Gonzalez[156], M.J. Costa[165], F. Costanza[4], D. Costanzo[142], J. Couthures[4], G. Cowan[95], K. Cranmer[172], L. Cremer[48], D. Cremonini[24b,24a], S. Crépé-Renaudin[59], F. Crescioli[128], T. Cresta[72a,72b], M. Cristinziani[144], M. Cristoforetti[77a,77b], T. M. Critchley[55], E. Critelli[96], A. Cueto[99], H. Cui[96], Z. Cui[7], B.M. Cunnett[149], W.R. Cunningham[58], E. Cuppini[110], F. Curcio[165], J. R. Curran[51], G. D'amen[30], V. D'Amico[109], M. D'Andrea[56b,56a], G. D'anniballe[73a,73b], S. D'Auria[70a,70b], A. D'Avanzo[71a,71b], L. D'Eramo[40], A. D'Onofrio[71a,71b], M. D'Onofrio[92], M. D'uffizi[101], M.J. Da Cunha Sargedas De Sousa[56b,56a], J.V. Da Fonseca Pinto[81b], C. Da Via[101], W. Dabrowski[85a], T. Dado[37], S. Dahbi[151], T. Dai[106], D. Dal Santo[20], C. Dallapiccola[103], M. Dam[42], J.R. Dandoy[35], D. Dannheim[37], M. Danninger[145], V. Dao[148], G. Darbo[56b], F. Dattola[47], T. Davidek[134], J. Davidson[169], I. Dawson[94], K. De[8], C. De Almeida Rossi[158], N. De Biase[47], S. De Castro[24b,24a], N. De Groot[115], P. de Jong[116], H. De la Torre[117], A. De Maria[112a], S. De Miranda Rimes[81d], A. De Salvo[74a], U. De Sanctis[75a,75b], F. De Santis[69a,69b], A. De Santo[149], J.B. De Vivie De Regie[59], K.G. De Vries[116], J. Debevc[93], D.V. Dedovich[38], J. Degens[92], A.M. Deiana[44], J. Del Peso[99], L. Delagrange[27], F. Deliot[136], C.M. Delitzsch[48], A. Dell'Acqua[37], L. Dell'Asta[70a,70b], M. Della Pietra[71a,71b], D. Della Volpe[55], M. Delmastro[4], C.C. Delogu[56b,56a], P.A. Delsart[59], S. Demers[174], M. Demichev[38], H. Denizli[22a,p], M.G. Depala[92], D. Derendarz[86], L. Derin[56b,56a], F. Derue[128], P. Dervan[92,†], A. M. Desai[1], K. Desch[25], F.A. Di Bello[73a,73b], A. Di Ciaccio[75a,75b], L. Di Ciaccio[4], D. Di Croce[37], C. Di Donato[71a,71b], A. Di Girolamo[37], G. Di Gregorio[65], A. Di Luca[77a,77b], B. Di Micco[76a,76b], R. Di Nardo[76a,76b], K.F. Di Petrillo[39], M. Diamantopoulou[154], F.A. Dias[116], M.A. Diaz[138a,138b], A. R. Didenko[38], M. Didenko[165], S.D. Diefenbacher[18a], E.B. Diehl[106], S. Díez Cornell[47], C. Diez Pardos[144], C. Dimitriadi[147], A. Dimitrievska[21], A. Dimri[148], Y. Ding[61], J. Dingfelder[25], T. Dingley[127], I-M. Dinu[28b], S.J. Dittmeier[62b], F. Dittus[37], M. Divisek[134], B. Dixit[92], F. Djama[102], T. Djobava[152b], C. Doglioni[101,98], A. Dohnalova[29a], Z. Dolezal[134], K. Domijan[85a], K.M. Dona[39], M. Donadelli[81d], B. Dong[107], J. Donini[40], J. Dopke[135], A. Doria[71a], N. Dos Santos Fernandes[131a],

JHEP10(2026)027

I.A. Dos Santos Luz[81e], P. Dougan[44], M.T. Dova[90], A.T. Doyle[58], M.P. Drescher[54], E. Dreyer[171], I. Drivas-koulouris[10], M. Drnevich[118], D. Du[61], T. Du[39], T.A. du Pree[116], Z. Duan[112a], M. Dubau[4], F. Dubinin[38], M. Dubovsky[29a], E. Duchovni[171], G. Duckeck[109], P. K. Duckett[96], O.A. Ducu[28b], D. Duda[51], A. Dudarev[37], M.M. Dudek[86], E. R. Duden[27], L. Duflot[65], M. Dührssen[37], I. Duminica[28g], A.E. Dumitriu[28b], M. Dunford[62a], T. Duong[4], A. Duperrin[102], A.F. Duque Bran[40], H. Duran Yildiz[3a], A. Durglishvili[152b], G.I. Dyckes[18a], M. Dyndal[85a], B.S. Dziedzic[37], G.H. Eberwein[127], B. Eckerova[29a], J.C. Egan[96], S. Eggebrecht[54], E. Egidio Purcino De Souza[81e], G. Eigen[17], K. Einsweiler[18a], T. Ekelof[163], P.A. Ekman[98], S. El Farkh[36b], Y. El Ghazali[61], H. El Jarrari[104], A. El Moussaouy[36a], I. Elbaz[154], D. Elitez[37], M. Ellert[163], F. Ellinghaus[173], T.A. Elliot[95], J. Elmsheuser[30], M. Elsawy[83b], M. Elsing[37], D. Emeliyanov[135], Y. Enari[82], S. Epari[108], D. Ernani Martins Neto[86], F. Ernst[37], M. Escalier[65], C. Escobar[165], R. Estevam De Paula[81c], E. Etzion[154], G. Evans[131a,131b], H. Evans[67], L.S. Evans[47], S. Ezzarqtouni[36a], F. Fabbri[24b,24a], L. Fabbri[24b,24a], G. Facini[96], V. Fadeyev[137], D. Fakoudis[100], S. Falciano[74a], L.F. Falda Ulhoa Coelho[27], F. Fallavollita[110], G. Falsetti[43b,43a], J. Faltova[134], C. Fan[164], K. Y. Fan[63b], Y. Fan[14], Y. Fang[14,112c], M. Fanti[70a,70b], M. Faraj[68a,68c], Z. Farazpay[97], A. Farbin[8], A. Farilla[76a], K. Farman[151], J. N. Farr[174], M. S. Farrington[60], S.M. Farrington[135,51], F. Fassi[36e], D. Fassouliotis[9], L. Fayard[65], G. Fazzino[62b], P. Federic[134], P. Federicova[132], M. Feickert[172], L. Feligioni[102], D.E. Fellers[18a], C. Feng[113b], Y. Feng[14], Z. Feng[65], B. Fernandez Barbadillo[91], P. Fernandez Martinez[66], C. Fernandez Ruiz[33], J. Ferrando[91], A. Ferrari[163], P. Ferrari[116,115], R. Ferrari[72a], D. Ferrere[55], C. Ferretti[106], M. P. Fewell[1], D. Fiacco[74a,74b], F. Fiedler[100], P. Fiedler[133], S. Filimonov[38], M.S. Filip[28b,q], A. Filipčič[93], M. Filipig[68a,68c], E.K. Filmer[159a], F. Filthaut[115], M.C.N. Fiolhais[131a,131c,r], L. Fiorini[165], W.C. Fisher[107], T. Fitschen[101], I. Fleck[144], P. Fleischmann[106], T. Flick[173], M. Flores[34d,s], L.R. Flores Castillo[63a], M. Foll[126], F.M. Follega[77a,77b], N. Fomin[33], A. Formica[136], M. Fornasiero[149], A.C. Forti[101], N. Forti[24b,24a], E. Fortin[102], A.W. Fortman[18a], L. Foster[18a], L. Fountas[9], H. Fox[91], P. Francavilla[73a,73b], S. Francescato[60], S. Franchellucci[20], M. Franchini[24b,24a], S. Franchino[62a], D. Francis[37], L. Franco[47], L. Franconi[47], M. Franklin[60], G. Frattari[37], Y.Y. Frid[154], N. Fritzsche[37], A. Froch[55], D. Froidevaux[37], J.A. Frost[135], Y. Fu[107], S. Fuenzalida Garrido[138g], Y.C. Fujikake[137], M. Fujimoto[148], K. Y. Fung[63a], E. Furtado De Simas Filho[81e], M. Furukawa[156], M. Fuste Costa[47], P. Fuste Martin[13], J. Fuster[165], A. Gaa[54], A. Gabrielli[24b,24a], A. Gabrielli[158], G. Gagliardi[56b,56a], L.G. Gagnon[146], S. Galantzan[154], J. Gallagher[1], E.J. Gallas[127], A.L. Gallen[163], B.J. Gallop[135], K.K. Gan[120], Y. Gao[51], Z. Gao[112a], A. Garabaglu[140], F.M. Garay Walls[138a,138b], C. García[165], A. Garcia Alonso[116], A.G. Garcia Caffaro[174], J.E. García Navarro[165], M. A. Garcia Ruiz[23b], M. Garcia-Sciveres[18a], G.L. Gardner[129], R.W. Gardner[39], N. Garelli[161], R.B. Garg[146], J.M. Gargan[33], C.A. Garner[158], C.M. Garvey[34a], V. K. Gassmann[161], G. Gaudio[72a], A.J. Gavin[94], J. Gavranovic[93], I.L. Gavrilenko[131a], C. Gay[166], G. Gaycken[124], A. Gekow[120], C. Gemme[56b], M.H. Genest[59], A. D. Gentry[114], S. George[95], T. Geralis[45], A. A. Gerwin[121], P. Gessinger-Befurt[37], M. Ghani[169], K. Ghorbanian[94], A. Ghosal[144], A. Ghosh[162], A. Ghosh[7], B. Giacobbe[24b], S. Giagu[74a,74b], A. Giannini[61], S.M. Gibson[95],

JHEP10(2026)027

D.T. Gil[85b], B.J. Gilbert[41], D. Gillberg[35], G. Gilles[116], D.M. Gingrich[2,t], M.P. Giordani[68a,68c], P.F. Giraud[136], G. Giugliarelli[68a,68c], D. Giugni[70a], F. Giuli[75a,75b,u], I. Gkialas[9,v], B.C. Gladwyn[127], C. Glasman[99], M. Glazewska[20], R. M. Gleason[162], G. Glemža[47], I. Gnesi[24b,24a,w], Y. Go[30], M. Goblirsch-Kolb[37], B. Gocke[48], D. Godin[108], B. Gokturk[22a], S. Goldfarb[105], T. Golling[55], M.G.D. Gololo[34c], A. Golub[140], J.P. Gombas[107], A. Gomes[131a,131b], G. Gomes Da Silva[144], A.J. Gomez Delegido[37], R. Gonçalo[131a], A. Gongadze[152c], F. Gonnella[21], J.L. Gonski[146], R.Y. González Andana[51], S. González de la Hoz[165], M. V. Gonzalez Rodrigues[47], R. Gonzalez Suarez[163], S. Gonzalez-Sevilla[55], L. Goossens[37], B. Gorini[37], E. Gorini[69a,69b], A. Gorišek[93], T.C. Gosart[129], A.T. Goshaw[50], M.I. Gostkin[38], S. Goswami[122], C.A. Gottardo[37], S. A. Gotz[109], M. Gouighri[36b], A.G. Goussiou[140], N. Govender[34c], R. P. Grabarczyk[127], I. Grabowska-Bold[85a], K. Graham[35], E. Gramstad[126], S. Grancagnolo[69a,69b], C.M. Grant[1], P.M. Gravila[28f], F.G. Gravili[69a,69b], H.M. Gray[18a], M. Greco[110], M. J. Green[1], C. Grefe[25], A. S. Grefsrud[37], I.M. Gregor[47], K.T. Greif[162], P. Grenier[146], S.G. Grewe[110], K. Grimm[32], S. Grinstein[13,x], E. Gross[171], J. Grosse-Knetter[54], L.H. Grossman[18b], L. Guan[106], W. Guérin[89], G. Guerrieri[37], R. Guevara[126], R. Gugel[100], J.A.M. Guhit[106], A. Guida[19], E. Guilloton[169], S. Guindon[37], F. Guo[14,112c], J. Guo[141a], L. Guo[47], L. Guo[112b,y], Y. Guo[106], Y. Guo[41], A. Gupta[48], R. Gupta[130], S. Gupta[27], S. Gurbuz[25], S.S. Gurdasani[47], G. Gustavino[74a,74b], P. Gutierrez[121], L.F. Gutierrez Zagazeta[129], M. Gutsche[49], C. Gutschow[96], C. Gwenlan[127], C.B. Gwilliam[92], E.S. Haaland[126], A. Haas[118], M. Habedank[58], C. Haber[18a], R.J. Haberle[171], H.K. Hadavand[8], A. Haddad[40], A. Hadef[49], A.I. Hagan[91], J. J. Hahn[144], M. Haleem[168], J. Haley[122], G.D. Hallewell[102], J.A. Hallford[47], H. Hamdaoui[163], M. Hamer[25], S. E. D. Hammoud[65], E.J. Hampshire[95], L. Han[112a], L. Han[61], S. Han[14], K. Hanagaki[82], M. Hance[137], D.A. Hangal[41], H. Hanif[145], M.D. Hank[129], J.B. Hansen[42], P.H. Hansen[42], T. Harenberg[173], S. Harkusha[175], M.L. Harris[103], Y.T. Harris[25], J. Harrison[13], P.F. Harrison[169], M. L. E. Hart[96], N.M. Hartman[110], N.M. Hartmann[109], R. Z. Hasan[95,135], Y. Hasegawa[143], D. Hashimoto[111], F. Haslbeck[37], S. Hassan[126], R. Hauser[107], M. Haviernik[134], C.M. Hawkes[21], R.J. Hawkings[37], Y. Hayashi[156], D. Hayden[107], R.L. Hayes[116], C.P. Hays[127], J.M. Hays[94], H.S. Hayward[92], M. He[14,112c], Y. He[47], Y. He[96], V. Hedberg[98], J. Heilman[35], S. Heim[47], T. Heim[18a], J.J. Heinrich[124], L. Heinrich[110], J. Hejbal[132], M. Helbig[49], A. Held[172], S. Hellesund[17], C.M. Helling[166], F.N.E. Henry[58], H. Herde[98], Y. Hernández Jiménez[148], G. Herten[53], R. Hertenberger[109], L. Hervas[37], M.E. Hesping[100], N.P. Hessey[159a], J. Hessler[110], R. Hicks[129], M. Hidaoui[36b], N. Hidic[134], E. Hill[158], T. S. Hillersoy[17], S.J. Hillier[21], J.R. Hinds[107], F. Hinterkeuser[25], M. Hirose[125], S. Hirose[170], D. Hirschbuehl[173], B. Hiti[93], J. Hobbs[148], R. Hobincu[28e], N. Hod[171], A.M. Hodges[164], M.C. Hodgkinson[142], B.H. Hodkinson[127], A. Hoecker[37], D. D. Hofer[106], J. Hofer[165], J. Hofner[100], M. Holzbock[37], L.B.A.H. Hommels[33], V. Homsak[127], J. J. Hong[67], T.M. Hong[130], R. Honscheid[127], B.H. Hooberman[164], W.H. Hopkins[6], M. C. Hoppesch[164], Y. Horii[111], M. E. Horstmann[110], M.M. Horzela[54], S. Hou[151], M. R. Housenga[164], J. Howarth[58], J. Hoya[6], M. Hrabovsky[123], T. Hryn'ova[4], P.J. Hsu[64], S.-C. Hsu[140], T. Hsu[65], M. Hu[18a], P. Hu[63b], Q. Hu[61], S. Huang[33], X. Huang[14,112c], Y. Huang[134],

JHEP10(2026)027

Y. Huang[112b], Y. Huang[14], Z. Huang[65], Z. Hubacek[133], F. Huegging[25], T.B. Huffman[127], M. Hufnagel Maranha De Faria[81a], C. A. Hugli[47], M. Huhtinen[37], S.K. Huiberts[17], R. Hulsken[104], C. E. Hultquist[18a], D.L. Humphreys[103], N. Huseynov[12], J. Huston[107], B. Huth[37], J. Huth[60], L. Huth[47], R. Hyneman[7], G. Iacobucci[55], G. Iakovidis[30], L. Iconomidou-Fayard[65], J. P. Iddon[37], P. Iengo[71a,71b], Y. Iiyama[156], T. Iizawa[156], Y. Ikegami[82], D. Iliadis[155], N. Ilic[158], H. Imam[36a], G. Inacio Goncalves[81d], S. A. Infante Cabanas[138c], T. Ingebretsen Carlson[46a,46b], J. M. Inglis[94], G. Introzzi[72a,72b], M. Iodice[76a], V. Ippolito[74a,74b], R. K. Irwin[92], M. Ishino[156], W. Islam[172], C. Issever[19], O. N. Istaitia[65,f], S. Istin[22a,z], K. Itabashi[125], H. Ito[170], R. Iuppa[77a,77b], A. Ivina[171], F. Ivone[37], S. Izumiyama[111], V. Izzo[71a], P. Jacka[133], P. Jackson[1], P. R. Jacobson[50], P. Jain[47], K. Jakobs[53], J. Jamieson[58], W. Jang[156], S. Jankovych[116], B. K. Jashal[135], M. Javurkova[103], P. Jawahar[101], L. Jeanty[124], J. Jejelava[152a,aa], P. Jenni[53,ab], L. Jerala[93], C.E. Jessiman[35], H. Jia[166], J. Jia[148], K. Jia[146], X. Jia[110,112c], C. Jiang[51], Q. Jiang[63b], S. Jiggins[47], M. Jimenez Ortega[165], J. Jimenez Pena[13], S. Jin[112a], A. Jinaru[28b], O. Jinnouchi[139], P. Johansson[142], K.A. Johns[7], J.W. Johnson[137], F. A. Jolly[47], D.M. Jones[149], E. Jones[47], P. Jones[33], R.W.L. Jones[91], T.J. Jones[92], H.L. Joos[37], R. Joshi[120], J. Jovicevic[16], X. Ju[18a], J.J. Junggeburth[37], T. Junkermann[62a], A. Juste Rozas[13,x], M.K. Juzek[86], S. Kabana[138f], A. Kaczmarska[86], S. A. Kadir[146], M. Kado[110], H. Kagan[120], M. Kagan[146], A. Kahn[129], C. Kahra[100], T. Kaji[156], E. Kajomovitz[153], N. Kakati[171], N. Kakoty[13], S. Kandel[8], E. Kanellaki[45], N. Kanellos[10], S. Kang[50], D. Kar[34j,†], E. Karentzos[25], K. Karki[8], O. Karkout[116], S.N. Karpov[38], Z.M. Karpova[38], V. Kartvelishvili[91,152b], E. Kasimi[155], J. Katzy[47], S. Kaur[35], R. Kavak[37], K. Kawade[143], M.P. Kawale[121], C. Kawamoto[87], E.F. Kay[37], S. Kazakos[107], K. Kazakova[102], J.M. Keaveney[34a], R. Keeler[167], G.V. Kehris[60], J.S. Keller[35], J. M. Kelly[167], J.I. Kelsey[164], J.J. Kempster[149], O. Kepka[132], J. Kerr[159b], B.P. Kerridge[135], B.P. Kerševan[93], L. Keszeghova[29a], M.B. Khan[93], R. A. Khan[130], A. Khanov[122], M. Kholodenko[131a], T.J. Khoo[19], G. Khoriauli[168], Y. Khoulaki[36a], Y.A.R. Khwaira[128], D. Kim[6], D.W. Kim[18b], Y.K. Kim[39], N. Kimura[96], M.K. Kingston[54], F. Kirfel[25], J. Kirk[135], A.E. Kiryunin[110], S. Kita[156], O. Kivernyk[25], M. Klassen[37], C. Klein[35], L. Klein[168], M.H. Klein[44], U. Klein[92], A. Klimentov[30], P. Kluit[116], S. Kluth[110], E. Kneringer[78], T.M. Knight[158], A. Knue[48], M. Kobel[49], D. Kobylianskii[171], S.F. Koch[37], M. Kocian[146], P. Kodyš[134], D.M. Koeck[124], T. Koffas[35], K. Kojima[82], O. Kolay[49], I. Koletsou[4], T. Komarek[86], S. Kondo[156], K. Köneke[54], A.X.Y. Kong[1], T. Kono[119], N. Konstantinidis[96], P. Kontaxakis[55], B. Konya[98], R. Kopeliansky[41], S. Koperny[85a], R. Koppenhofer[53], I. Kopsalis[10], K. Korcyl[86], K. Kordas[155,ac], A. Korn[96], S. Korn[54], I. Korolkov[13], O. Kortner[110], S. Kortner[110], W.H. Kostecka[117], M. Kostov[29a], V.V. Kostyukhin[144], A. Kotsokechagia[37], A. Kotwal[50], A. Koulouris[37], A. Kourkoumeli-Charalampidi[72a,72b], O. Kovanda[124], R. Kowalewski[167], W. Kozanecki[124], G. Kramberger[93], P. Kramer[25], A. Krasznahorkay[103], A. C. Kraus[117], J.W. Kraus[173], J.A. Kremer[47], N. B. Krengel[144], T. Kresse[158], L. Kretschmann[173], J. Kretzschmar[92], P. Krieger[158], K. Krizka[21], K. Kroeninger[48], H. Kroha[110], J. Kroll[132], J. Kroll[129], K.S. Krowpman[107], U. Kruchonak[38], H. Krüger[25], N. Krumnack[79], J. Krupa[146], M.C. Kruse[50], O. Kuchinskaia[38], S. Kuday[3a], S. Kuehn[37], R. Kuesters[53],

JHEP10(2026)027

T. Kuhl[47], V. Kukhtin[38], Y. Kulchitsky[38], S. Kuleshov[138d,138b], J. Kull[1], E. V. Kumar[109], M. Kumar[34j], N. Kumari[47], P. Kumari[159b], A. Kupco[132], O. Kuprash[53], H. Kurashige[84], L.L. Kurchaninov[159a], O. Kurdysh[4], M. Kuze[139], A.K. Kvam[103], J. Kvita[123], N.G. Kyriacou[140], M. Laassiri[30], C. Lacasta[165], H. Lacker[19], D. Lacour[128], E. Ladygin[38], A. Lafarge[40], B. Laforge[128], T. Lagouri[174], F.Z. Lahbabi[36a], S. Lai[54], W. S. Lai[96], I.K. Lakomiec[54], J.E. Lambert[167], S. Lammers[67], W. Lampl[7], C. Lampoudis[155], G. Lamprinoudis[168], A.N. Lancaster[117], U. Landgraf[53], M.P.J. Landon[94], V.S. Lang[53], A.J. Lankford[162], F. Lanni[37], C. S. Lantz[164], K. Lantzsch[25], A. Lanza[72a], M. Lanzac Berrocal[165], T. Lari[70a], D. Larsen[17], L. Larson[11], F. Lasagni Manghi[24b], M. Lassnig[37], H.C. Lau[167], S.D. Lawlor[142], R. Lazaridou[162], M. Lazzaroni[70a,70b], E. T. T. Le[162], H. D. M. Le[107], E.M. Le Boulicaut[174], D.O. Le Guennec[136], L.T. Le Pottier[18a], B. Leban[24b,24a], F. Ledroit-Guillon[59], T.F. Lee[159b], L.L. Leeuw[34h], M. Lefebvre[167], C. Leggett[18a], L.M. Lehmann[116], W.A. Leight[103], W. Leinonen[115], A. Leisos[155,ad], M.A.L. Leite[81c], C.E. Leitgeb[19], R. Leitner[134], E. Lelak[134], K.J.C. Leney[44], T. Lenz[25], S. Leone[73a], C. Leonidopoulos[51], A. Leopold[147], J. LePage-Bourbonnais[35], R. Les[65], C.G. Lester[33], J. Levêque[4], L.J. Levinson[171], G. Levrini[24b,24a], M.P. Lewicki[86], C. Lewis[140], D.J. Lewis[4], L. Lewitt[142], A. Li[30], B. Li[113b], C-Q. Li[110], C. Li[106], H. Li[113b], H. Li[101], H. Li[15], H. Li[61], H. Li[113b], J. Li[141a], L. Li[141a], R. Li[174], S. Li[141b,141a], Y. Li[14], Z. Li[14,112c], Z. Li[61], S. Liang[14,112c], Z. Liang[14], M. Liberatore[136], B. Liberti[75a], G. B. Libotte[81d], K. Lie[63c], J. Lieber Marin[81e], H. Lien[67], H. Lin[106], S. F. Lin[148], L. Linden[109], R.E. Lindley[7], J.H. Lindon[37], J. Ling[60], E. Lipeles[129], A. Lipniacka[17], A. Lister[166], J.D. Little[67], B. Liu[113a], B.X. Liu[112b], D. Liu[153], D. Liu[137], E. H. L. Liu[21], H. Liu[112b], J.K.K. Liu[118], K. Liu[141b], K. Liu[141b], M. Liu[61], M.Y. Liu[61], P. Liu[113b], Q. Liu[146], S. Liu[148], X. Liu[113b], Y. Liu[112b,112c], Y. Liu[164], Y.L. Liu[113b], Y.W. Liu[61], Z. Liu[65,ae], S.L. Lloyd[94], E.M. Lobodzinska[47], P. Loch[7], E. Lodhi[158], K. Lohwasser[142], E. Loiacono[122], J. D. Lomas[21], I. Longarini[162], R. Longo[24b,24a,w], A. Lopez Solis[13], N.A. Lopez-canelas[7], N. Lorenzo Martinez[4], A.M. Lory[109], M. Losada[83b], G. Löschcke Centeno[4], X. Lou[14,112c], P.A. Love[91], H. Lu[14], M. Lu[65], S. Lu[129], Y.J. Lu[151], H.J. Lubatti[140], C. Luci[74a,74b], F.L. Lucio Alves[112a], J.A. Lue[124], F. Luehring[67], B. S. Lunday[129], O. Lundberg[147], J. Lunde[37], N.A. Luongo[6], M.S. Lutz[158], A.B. Lux[26], D. Lynn[30], R. Lysak[132], V. Lysenko[133], E. Lytken[98], V. Lyubushkin[38], T. Lyubushkina[38], M.M. Lyukova[148], H. Ma[30], K. Ma[61], L.L. Ma[113b], W. Ma[61], Y. Ma[113b], B. Maček[93], P.C. Machado De Abreu Farias[81e], D. Macina[37], R. Madar[40], T. Madula[96], J. Maeda[84], T. Maeno[30], P.T. Mafa[34f], G. Magni[65], H. Maguire[142], M. Maheshwari[33], V. Maiboroda[65], G. Maineri[70a,70b], A. Maio[131a,131b,131d], K. Maj[85a], O. Majersky[47], S. Majewski[124], A. Makita[156], N. Makovec[65], V. Maksimovic[16], B. Malaescu[128], J. Malamant[126], Pa. Malecki[86], F. Malek[59,af], M. Mali[93], D. Malito[95], A. Maloizel[5], A. Malvezzi Lopes[81d], S. Malyukov[38], J. Mamuzic[93], G. Mancini[52], M. N. Mancini[27], G. Manco[72a,72b], S.S. Mandarry[149], I. Mandić[93], L. Manhaes de Andrade Filho[81a], I.M. Maniatis[171], J. Manjarres Ramos[89], D.C. Mankad[171], A. Mann[109], T. Manoussos[100], M.N. Mantinan[39], S. Manzoni[37], L. Mao[141a], X. Mapekula[34c], A. Marantis[155], R.R. Marcelo Gregorio[1], G. Marchiori[5], C. Marcon[70a],

JHEP10(2026)027

E. Maricic[16], M. Marinescu[47], S. Marium[47], M. Marjanovic[121], A. Markhoos[53], M. Markovitch[65], M. K. Maroun[103], M. C. Marr[145], T. L. Marsault[136], G. T. Marsden[101], Z. Marshall[18a], S. Marti-Garcia[165], J. Martin[96], T.A. Martin[135], V.J. Martin[51], B. Martin dit Latour[17], S. Martin-Haugh[135], F. Martina[69a,69b], L. Martinelli[74a,74b], V.I. Martinez Outschoorn[103], P. Martinez Suarez[37], G. Martinovicova[134], V.S. Martoiu[28b], A. Martone[89], A.C. Martyniuk[96], A. Marzin[37], D. Mascione[77a,77b], L. Masetti[100], J. Masik[101], A.L. Maslennikov[38], S.L. Mason[41], P. Massarotti[71a,71b], P. Mastrandrea[73a,73b], A. Mastroberardino[43b,43a], R. Mastrofrancesco[72a,72b], T. Masubuchi[125], T.T. Mathew[124], J. Matousek[134], D.M. Mattern[48], K. Mauer[47], J. Maurer[28b], T. Maurin[58], C. Mavungu Tsava[102], A. E. May[101], E. Mayer[40], R. Mazini[34j], S.M. Mazza[137], E. Mazzeo[37], J.P. Mc Gowan[167], S.P. Mc Kee[106], C.C. McCracken[166], E.F. McDonald[105], L. F. Mcelhinney[91], J.A. Mcfayden[149], R.P. McGovern[167], R.P. Mckenzie[34j], D.J. Mclaughlin[96], S.J. McMahon[135], C.M. Mcpartland[92], R.A. McPherson[167,o], S. Mehlhase[109], A. Mehta[92], D. Melini[165], B.R. Mellado Garcia[14,ag], A.H. Melo[54], F. Meloni[47], A.M. Mendes Jacques Da Costa[101], L. Meng[91], S. Menke[110], M. Mentink[37], E. Meoni[43b,43a], G. Mercado[117], S. Merianos[155], C. Merlassino[68a,68c], C. Meroni[70a,70b], J. Metcalfe[6], A.S. Mete[6], E. Meuser[100], C. Meyer[67], J-P. Meyer[136], O. Mezhenska[29b], Y. Miao[112a], R.P. Middleton[135], M. Mihovilovic[65], L. Mijović[51], G. Mikenberg[171], M. Mikestikova[132], M. Mikuž[93], H. Mildner[100], A. Milic[37], D.W. Miller[39], E. H. Miller[146], A. Milov[171], D.A. Milstead[46a,46b], T. Min[112a], I.A. Minashvili[152b], A.I. Mincer[118], B. Mindur[85a], M. Mineev[38], L.M. Mir[13], M. Miralles Lopez[58], M. Mironova[18a], M. Missio[40], A. Mitra[169], V.A. Mitsou[165], P.S. Miyagawa[94], R. Mizuhiki[84], T. Mkrtchyan[37], M. Mlinarevic[96], T. Mlinarevic[96], M. Mlynarikova[134], L. Mlynarska[85a], C. Mo[141a], H. Möbius[47], S. Mobius[20], M. H. Mohamed Farook[114], S. Mohapatra[41], M.F. Mohd Soberi[51], S. Mohiuddin[122], G. Mokgatitswane[34j], R. Mole[21], L. Moleri[171], U. Molinatti[127], M. E. Mollerach[31], L.G. Mollier[20], L. Monaco[37,58], B. Mondal[132], S. Mondal[134], K. Mönig[47], E. Monnier[102], L. Monsonis Romero[165], A. Montella[46a,46b], M. Montella[120], F. Montereali[76a,76b], F. Monticelli[90], S. Monzani[68a,68c], M.E.E. Moors[25], A. Morancho Tarda[42], N. Morange[65], M. Moreno Llácer[165], C. Moreno Martinez[55], J.M. Moreno Perez[23b], P. Morettini[56b], S. Morgenstern[62a], M. Morii[60], M. Morinaga[156], F. Morodei[74a,74b], P. Moschovakos[37], B. Moser[53], M. Mosidze[152b], T. Moskalets[44], P. Moskvitina[115], C.J. Mosomane[34b], J. Moss[32], T. Motta Quirino[81d], A. Moussa[36d], Y. Moyal[171,ah], H. Moyano Gomez[13], E.J.W. Moyse[103], T.G. Mroz[86], S. Muanza[102], M. Mucha[25], J. Mueller[130], D. Muller[144], G.A. Mullier[163], A.J. Mullin[33], J.J. Mullin[50], A.C. Mullins[44], A.E. Mulski[60], D.P. Mungo[158], D. Munoz Perez[122], F.J. Munoz Sanchez[101], W.J. Murray[169,135], E. Musajan[61], M. Muškinja[93], C. Mwewa[47], A.J. Myers[8], G. Myers[106], M. Myska[133], B.P. Nachman[146], I.A. Nadas[28d], K. Nagai[127], K. Nagano[82], R. Nagasaka[156], J.L. Nagle[30,ai], E. Nagy[102], A.M. Nairz[37], T. Nakagawa[87], Y. Nakahama[82], K. Nakamura[82], A. Nandi[62b], H. Nanjo[125], E.A. Narayanan[44], Y. Narukawa[156], L. Nasella[70a,70b], S. Nasri[83c], C. Nass[25], G. Navarro[23a], A. Nayaz[19], S. Nechaeva[24b,24a], F. Nechansky[132], L. Nedic[127], A. Negri[72a,72b], M. Negrini[24b], C. Nellist[116], C. Nelson[104], K. Nelson[106], S. Nemecek[132], M. Nessi[37,e], M.S. Neubauer[164], J. Newell[92], P.R. Newman[21], Y.W.Y. Ng[164], B. Ngair[83b],

JHEP10(2026)027

H.D.N. Nguyen[108], J.D. Nichols[121], R. Nicolaidou[136], J. Nielsen[137], M. Niemeyer[54], J. Niermann[37], N. Nikiforou[37], I. Nikolic-Audit[128], P. Nilsson[30], G. Ninio[154], A. Nisati[74a], D. Nishimura[156], R. Nisius[110], N. Nitika[171], E.K. Nkadimeng[34b], T. Nobe[156], D. Noll[146], T. Nommensen[150], M.B. Norfolk[142], B.J. Norman[35], L.C. Nosler[18a], M. Noury[36a], J. Novak[93], T. Novak[93], P. Novotny[171], R. Novotny[133], L. Nozka[123], K. Ntekas[37], D. Ntounis[146], N.M.J. Nunes De Moura Junior[81b], A.P. O'Neill[20], J. Ocariz[128], I. Ochoa[131a], A. Odella Rodriguez[13], S. Oerdek[47], J.T. Offermann[39], A. Ogrodnik[86], A. Oh[101], C.C. Ohm[147], H. Oide[82], M.L. Ojeda[37], Y. Okumura[156], L.F. Oleiro Seabra[131a], I. Oleksiyuk[55], G. Oliveira Correa[13], D. Oliveira Damazio[30], J.L. Oliver[1], R. Omar[67], Y. Onoda[139], A. Onofre[131a,131e,aj], P.U.E. Onyisi[11], M.J. Oreglia[39], D. Orestano[76a,76b], R. Orlandini[76a,76b], R.S. Orr[158], L.M. Osojnak[41], Y. Osumi[111], G. Otero y Garzón[31], H. Otono[88], M. Ouchrif[36d], F. Ould-Saada[126], T. Ovsiannikova[140], M. Owen[58], R.E. Owen[135], S.A. Oyeniran[114], V.E. Ozcan[22a], F. Ozturk[86], N. Ozturk[8], S. Ozturk[80], H.A. Pacey[127], K. Pachal[159a], A. Pacheco Pages[13], C. Padilla Aranda[13], G. Padovano[74a,74b], S. Pagan Griso[18a], L. Pagani[75a,75b], J. Pampel[25], D.K. Panchal[11], C.E. Pandini[59], J.G. Panduro Vazquez[135], H.D. Pandya[1], H. Pang[136], P. Pani[47], G. Panizzo[68a,68c], L. Panwar[128,ak], L. Paolozzi[21], S. Parajuli[164], A. Paramonov[6], C. Paraskevopoulos[52], D. Paredes Hernandez[63b], S.R. Paredes Saenz[51], A. Pareti[72a,72b], K.R. Park[41], T.H. Park[110], F. Parodi[56b,56a], J.A. Parsons[41], J.A. Partridge[137], U. Parzefall[53], B.A. Paschen[18a], B. Pascual Dias[40], L. Pascual Dominguez[99], E. Pasqualucci[74a], S. Passaggio[56b], F. Pastore[95], P. Patel[86], U.M. Patel[50], J.R. Pater[101], T. Pauly[37], A. Paunovic[16], F. Pauwels[134], C.I. Pazos[161], M. Pedersen[126], R. Pedro[131a], O. Penc[132], C.C. Penelaud[128], S. Peng[15], G. D. Penn[174], B.S. Peralva[81d], A.P. Pereira Peixoto[140], L. Pereira Sanchez[146], D.V. Perepelitsa[30,ai], G. Perera[103], E. Perez Codina[37], M. Perganti[10], H. Pernegger[37], S. Perrella[74a,74b], K. Peters[47], R.F.Y. Peters[101], B.A. Petersen[37], T.C. Petersen[42], E. Petit[102], V. Petousis[133], A. R. Petri[70a,70b], V.A. Petrovic[96], T. Petru[134], M. Pettee[18a], A. Petukhov[80], K. Petukhova[37], R. Pezoa[138g], L. Pezzotti[24b,24a], G. Pezzullo[174], L. Pfaffenbichler[37], A. J. Pfleger[78], T. Pham[105], T.M. Pham[172], P.W. Phillips[135], G. Piacquadio[148], E. Pianori[18a], F. Piazza[124], R. Piegaia[31], D. Pietreanu[28b], A.D. Pilkington[101], T. Pilusa[34j], M. Pinamonti[68a,68c], J.L. Pinfold[2], G. Pinheiro Matos[41], B.C. Pinheiro Pereira[131a], J. Pinol Bel[13], A. E. Pinto Pinoargote[128], L. Pintucci[68a,68c], K. M. Piper[149], A. Pirttikoski[55], D.A. Pizzi[35], L. Pizzimento[63b], A. Plebani[33], M.-A. Pleier[30], V. Pleskot[134], E. Plotnikova[38], G. Poddar[94], R. Poettgen[98], L. Poggioli[128], S. Polacek[134], G. Polesello[72a], A. Poley[145], A. Polini[24b], C.S. Pollard[169], Z.B. Pollock[120], E. Pompa Pacchi[121], N. I. Pond[96], D. Ponomarenko[67], L. Pontecorvo[37], S. Popa[28a], G.A. Popeneciu[28d], A. Poreba[37], D.M. Portillo Quintero[159a], S. Pospisil[133], M. A. Postill[142], P. Postolache[28c], K. Potamianos[169], P.A. Potepa[85a], I.N. Potrap[38], C.J. Potter[33], H. Potti[150], J. Poveda[165], M.E. Pozo Astigarraga[37], R. Pozzi[37], A. Prades Ibanez[75a,75b], S.R. Pradhan[142], J. Preston[95], J. Pretel[167], D. Price[101], M. Primavera[69a], L. Primomo[68a,68c], M.A. Principe Martin[99], R. Privara[123], T. Procter[85b], M.L. Proffitt[140], N. Proklova[129], K. Prokofiev[63c], G. Proto[110], J. Proudfoot[6], M. Przybycien[85a], W.W. Przygoda[85b], A. Psallidas[45], D. Pudzha[52], P. Puhl[57],

JHEP10(2026)027

H. I. Purnell[1], D. Pyatiizbyantseva[115], J. Qian[106], R. Qian[107], D. Qichen[127], Y. Qin[13], T. Qiu[51], A. Quadt[54], M. Queitsch-Maitland[101], G. Quetant[55], R.P. Quinn[166], D. Rafanoharana[110], J.L. Rainbolt[39], S. Rajagopalan[30], E. Ramakoti[38], L. Rambelli[56b,56a], I.A. Ramirez-Berend[35], K. Ran[106,112c], S. D. Randles[92], D. S. Rankin[129], N.P. Rapheeha[34j], H. Rasheed[28b], A. Rastogi[18a], S. Rave[100], S. Ravera[56b,56a], B. Ravina[37], I. Ravinovich[171], M. Raymond[37], A.L. Read[126], N.P. Readioff[142], D.M. Rebuzzi[72a,72b], A. S. Reed[58], K. Reeves[27], D. Reikher[37], T. Reisch[55], A. Rej[48], H. Ren[61], M. Renda[28b], F. Renner[47], A.G. Rennie[58], M. Repik[55], A.L. Rescia[43b,43a], S. Resconi[70a], M. Ressegotti[56b], S. Rettie[116], W.F. Rettie[35], M. M. Revering[33], O.L. Rezanova[38], P. Reznicek[134], H. Riani[36d], N. Ribaric[37], B. Ricci[68a,68c], E. Ricci[77a,77b], R. Richter[110], E. Richter-Was[85b], M. Ridel[128], S. Ridouani[36d], P. Riedler[37], E.M. Riefel[46a,46b], J. O. Rieger[116], M. Rimoldi[34c], L. Rinaldi[24b,24a], P. Rincke[163,54], G. Ripellino[163], I. Riu[13], J.C. Rivera Vergara[167], F. Rizatdinova[122], E. Rizvi[94], B.R. Roberts[39], S.S. Roberts[137], D. Robinson[33], A. Robson[58], A. Rocchi[75a,75b], C. Roda[73a,73b], F.A. Rodriguez[117], S. Rodriguez Bosca[37], Y. Rodriguez Garcia[23a], A.M. Rodríguez Vera[117], S. Roe[37], J.T. Roemer[37], O. Røhne[126], R.A. Rojas[37], Z. Rokavec[93], C.P.A. Roland[128], A. Romaniouk[78], E. Romano[72a,72b], M. Romano[24b], N. Rompotis[92], L. Roos[128], S. Rosati[74a], L. Roscher[47], B.J. Rosser[39], E. Rossi[127], E. Rossi[71a,71b], L.P. Rossi[60], L. Rossini[53], R. Rosten[120], M. Rotaru[28b], R. Roth[37], F. A. Rothen[55], D. Rousseau[65], D. Rousso[47], S. Roy-Garand[55], A. Rozanov[102], Z. M. A. Rozario[58], Y. Rozen[153], A. Rubio Jimenez[165], V.H. Ruelas Rivera[19], T.A. Ruggeri[1], A. Ruggiero[127], A. Ruiz-Martinez[165], A. Rummler[37], G.B. Rupnik Boero[37], N.A. Rusakovich[38], S. Ruscelli[48], H.L. Russell[167], G. Russo[137], J.P. Rutherfoord[7], S. Rutherford Colmenares[118], M. Rybar[134], P. Rybczynski[85a], A. Ryzhov[44], M. A. E. Saadawy[44], F. Safai Tehrani[74a], S. Saha[1], B. Sahoo[171], B. T. Saifuddin[121], M. Saimpert[136], I. Sainz Saenz Diez[62a], G.T. Saito[81c], M. Saito[156], T. Saito[156], A. Sala[70a,70b], O. T. Salin[65], A. Salnikov[146], J. Salt[165], A. Salvador Salas[154], F. Salvatore[149], A. Salzburger[37], D. Sammel[53], E. Sampson[91], D. Sampsonidis[155,ac], D. Sampsonidou[124], M.A.A. Samy[58], J. Sánchez[165], H. Sandaker[126], C.O. Sander[47], J.A. Sandesara[172], M. Sandhoff[173], C. Sandoval[23b], L. Sanfilippo[62a], D.P.C. Sankey[135], T. Sano[87], A. Sansar[22c], A. Sansoni[52], M. Santana Queiroz[18b], L. Santi[37], C. Santoni[40], G. Santoro[43b,43a], H. Santos[131a,131b], L. Santos Pereira Trigo[47], E. Sanzani[24b,24a], K.A. Saoucha[83d], J.G. Saraiva[131a,131d], J. Sardain[7], S. Sarkar[50], O. Sasaki[82], K. Sato[160], C. Sauer[37], E. Sauvan[4], P. Savard[158,t], M. Savic[164], R. Sawada[156], C. Sawyer[135], L. Sawyer[97], A. M. Sayed[27], C. Sbarra[24b], A. Sbrizzi[24b,24a], R. Scaglioni[72a,72b], T. Scanlon[96], J. Schaarschmidt[140], U. Schäfer[100], A.C. Schaffer[65,44], D. Schaile[109], R.D. Schamberger[148], C. Scharf[19], M.M. Schefer[20], D. Scheirich[134], M. Schernau[138f], C. Scheulen[55], C. Schiavi[56b,56a], M. Schioppa[43b,43a], S. Schlenker[37], T. Schlomer[54], J. Schmeing[173], C. R. Schmidt[49], E. Schmidt[110], M. A. Schmidt[173], K. Schmieden[25], C. Schmitt[100], N. Schmitt[100], S. Schmitt[47], N.A. Schneider[109], L. Schoeffel[136], A. Schoening[62b], P.G. Scholer[35], E. Schopf[144], M. Schott[25], S. Schramm[55], T. Schroer[55], H-C. Schultz-Coulon[62a], M. Schumacher[53], B.A. Schumm[137], Ph. Schune[136], H.R. Schwartz[7], A. Schwartzman[146], T.A. Schwarz[106], Ph. Schwemling[136],

JHEP10(2026)027

R. Schwienhorst[107], F.G. Sciacca[20], A. Sciandra[30], G. Sciolla[27], S. A. Scoville[130], F. Scuri[73a], C.D. Sebastiani[37], K. Sedlaczek[117], A. Sehrawat[138b], S.C. Seidel[114], B.D. Seidlitz[41], C. Seitz[47], J.M. Seixas[81b], G. Sekhniaidze[71a], L. Selem[128], N. Semprini-Cesari[24b,24a], A. Semushin[175], V. Senthilkumar[116], L. Serin[65], M. Sessa[71a,71b], H. Severini[121], F. Sforza[56b,56a], A. Sfyrla[55], Q. Sha[14], H. Shaddix[117], A.H. Shah[33], R. Shaheen[147], J.D. Shahinian[129], M. Shamim[37], L.Y. Shan[14], M. Shapiro[18a], A. Sharma[37], A.S. Sharma[166], P. Sharma[30], K. Shaw[149], S.M. Shaw[101], D. Shemyakin[171], Q. Shen[14], D.J. Sheppard[145], P. Sherwood[96], L. Shi[112b], X. Shi[14], E.B. Shields[171], S. Shimizu[82], S. Shirabe[88], M. Shiyakova[38,al], M.J. Shochet[39], D.R. Shope[126], S. Shrestha[120,am], I. Shreyber[38], M.J. Shroff[104], P. Sicho[132], A.M. Sickles[164], E. Sideras Haddad[34j], A. C. Sidley[116], A. Sidoti[24b], F. Siegert[49], Dj. Sijacki[16], F. Sili[61], J.M. Silva[51], I. Silva Ferreira[81b], M.V. Silva Oliveira[30], S.B. Silverstein[46a], S. Simion[65], R. Simoniello[37], E.L. Simpson[101], H. Simpson[149], L.R. Simpson[6], S. Simsek[80], S. Singh[30], S. N. Singh[27], S. Sinha[47], S. Sinha[101], M. Sioli[24b,24a], K. Sioulas[9], E. Sitnikova[47], J. Sjölin[46a,46b], A. Skaf[54], E. Skorda[21], P. Skubic[121], M. Slawinska[86], I. Slazyk[17], I. Sliusar[126], V. Smakhtin[171], B.H. Smart[135], S.Yu. Smirnov[138b], Y. Smirnov[34c], O. Smirnova[98], J.L. Smith[101], M. B. Smith[35], R. Smith[146], H. Smitmanns[100], M. Smizanska[91], K. Smolek[133], P. Smolyanskiy[133], A.A. Snesarev[38], H.L. Snoek[116], R. M. Snyder[50], S. Snyder[30], R. Sobie[167,o], A. Soffer[154], C.A. Solans Sanchez[37], E.Yu. Soldatov[38], U. Soldevila[165], A.A. Solodkov[34j], S. Solomon[27], A. Soloshenko[38], O.V. Solovyanov[40], P. Sommer[49], A. Sopczak[133], A.L. Sopio[51], F. Sopkova[29b], J. D. Sorenson[114], I.R. Sotarriva Alvarez[139], V. Sothilingam[62a], O. J. Soto Sandoval[138c,138b], S. Sottocornola[67], R. Soualah[83a], D. South[47], N. Soybelman[171], S. Spagnolo[69a,69b], A.S. Spellman[124], D. Sperlich[53], B. Spisso[71a,71b], L. Splendori[102], M. Spousta[134], E.J. Staats[35], R. Stamen[62a], E. Stanecka[86], W. Stanek-Maslouska[47], M.V. Stange[49], B. Stanislaus[18a], M.M. Stanitzki[47], G.H. Stark[137], J. Stark[89], P. Staroba[132], P. Starovoitov[83d], R. Staszewski[86], C. Stauch[109], G. Stavropoulos[45], A. Stefl[37], A. Stein[100], P. Steinberg[30], B. Stelzer[145,159a], H.J. Stelzer[130], O. Stelzer[159a], H. Stenzel[57], T.J. Stevenson[149], G.A. Stewart[47], G. Stoicea[28b], M. Stolarski[131a], S. Stonjek[110], A. Straessner[49], J. Strandberg[147], S. Strandberg[46a,46b], M. Stratmann[173], M. Strauss[121], T. Strebler[102], P. Strizenec[29b], R. Ströhmer[168], D.M. Strom[124], R. Stroynowski[44], A. Strubig[46a,46b], S.A. Stucci[30], B. Stugu[17], J. Stupak[121], N.A. Styles[47], D. Su[146], S. Su[61], X. Su[61], D. Suchy[29a], A. D. Sudhakar Ponnu[54], L. Sudit[171], Y. Sue[82], K. Sugizaki[129], D.M.S. Sultan[127], L. Sultanaliyeva[25], S. Sultansoy[3b], S. Sun[172], W. Sun[14], S. Sundar Raman[166], N. Sur[98], J.P. Surdutovich[120], N. Suri Jr[174], M.R. Sutton[149], M. Svatos[132], P. N. Swallow[33], S.N. Swatman[37], M. Swiatlowski[159a], A. Swoboda[37], I. Sykora[29a], M. Sykora[134], T. Sykora[134], D. Ta[100], K. Tackmann[47,an], A. Taffard[162], R. Tafirout[159a], Y. Takubo[82], M. Talby[102], N.M. Tamir[154], A. Tanaka[156], J. Tanaka[156], R. Tanaka[65], M. Tanasini[148], Z. Tao[166], S. Tapia Araya[138g], S. Tapprogge[100], A. Tarek Abouelfadl Mohamed[37], S. Tarem[153], K. Tariq[14], G. Tarna[37], G.F. Tartarelli[70a], M. J. Tartarin[141b], P. Tas[134], M. Tasevsky[132], E. Tassi[43b,43a], A.C. Tate[164], Y. Tayalati[36e,ao], G.N. Taylor[105], W. Taylor[159b], R.J. Taylor Vara[165], A.S. Tegetmeier[89], P. Teixeira-Dias[95], J.J. Teoh[158],

JHEP10(2026)027

K. Terashi[156], J. Terron[99], S. Terzo[13], M. Testa[52], R.J. Teuscher[158,o], A. Thaler[78], T. Theveneaux-Pelzer[102], J.P. Thomas[21], E.A. Thompson[18a], P.D. Thompson[21], E. Thomson[129], R. E. Thornberry[30], T.M. Thory-Rao[21], C.N. Thotamuna Wijewardhana[148], C. Tian[61], Y. Tian[55], V. Tikhomirov[80], Yu.A. Tikhonov[38], D. Timoshyn[134], E.X.L. Ting[1], P. Tipton[174], A. Tishelman-Charny[30], K. Todome[139], S. Todorova-Nova[134], L. Toffolin[68a,68c], M. Togawa[82], J. Tojo[88], S. Tokár[29a], O. Toldaiev[67], A. J. Toler[103], G. Tolkachev[102], M. Tomoto[82], L. Tompkins[146], E. Torrence[124], H. Torres[89], D. I. Torres Arza[138g], E. Torres Reoyo[165], E. Torró Pastor[165], M. Toscani[31], C. Tosciri[39], M. Tost[11], D.R. Tovey[142], T. Trefzger[168], P.M. Tricarico[13], A. Tricoli[30], I.M. Trigger[159a], S. Trincaz-Duvoid[128], D.A. Trischuk[167], A. Tropina[38], D. Truncali[75a,75b], L. Truong[34c], M. Trzebinski[86], A. Trzupek[86], F. Tsai[148], A. Tsiamis[155], P.V. Tsiareshka[38], S. Tsigaridas[159a], A. Tsirigotis[155,ad], V. Tsiskaridze[152a], E.G. Tskhadadze[152a], H. F. Tsoi[129], Y. Tsujikawa[87], V. Tsulaia[18a], K. Tsuri[119], D. Tsybychev[148], Y. Tu[63b], A. Tudorache[28b], V. Tudorache[28b], S. B. Tuncay[127], S. Turchikhin[56b,56a], I. Turk Cakir[3a], R. Turra[70a], T. Turtuvshin[38,ap], P.M. Tuts[41], Y. Uematsu[82], F. Ukegawa[160], P.A. Ulloa Poblete[138c,138b], G. Unal[37], A. Undrus[30], J. Urban[29b], P. Urrejola[138e], G. Usai[8], R. Ushioda[157], M. Usman[108], F. Ustuner[51], Z. Uysal[80], V. Vacek[133], B. Vachon[104], A. Vaitkus[96], C. Valderanis[109], E. Valdes Santurio[46a,46b], M. Valente[37], S. Valentinetti[24b,24a], A. Valero[165], E. Valiente Moreno[165], S. Valjee[94], A. Vallier[89], J.A. Valls Ferrer[165], D. R. Van Arneman[116], R. Van Den Broucke[128], A. Van Der Graaf[48], H. Z. Van Der Schyf[34j], P. Van Gemmeren[6], M. Van Rijnbach[37], S. Van Stroud[96], I. Van Vulpen[116], P. Vana[134], M. Vanadia[75a,75b], U. M. Vande Voorde[147], W. Vandelli[37], E.R. Vandewall[146], D. Vannicola[154], R. Vari[74a], M. Varma[174], E.W. Varnes[7], C. Varni[85a], D. Varouchas[65], L. Varriale[165], K.E. Varvell[150], M.E. Vasile[28b], A. Vasileiadou[9], L. Vaslin[82], M. D. Vassilev[146], A. Vasyukov[38], L. M. Vaughan[122], R. Vavricka[134], T. Vazquez Schroeder[13], J. Veatch[32], V. Vecchio[101], M.J. Veen[103], I. Veliscek[30], I. Velkovska[93], L.M. Veloce[158], F. Veloso[131a,131c], A.G. Veltman[51], S.H. Venetianer[161], S. Veneziano[74a], A. Ventura[69a,69b], A. Verbytskyi[110], M. Verducci[73a,73b], C. Vergis[94], M. Verissimo De Araujo[81b], W. Verkerke[116], J.C. Vermeulen[116], C. Vernieri[146], M. Vessella[162], M.C. Vetterli[145,t], A. Vgenopoulos[100], N. Viaux Maira[138g,aq], L. Vicenik[133], T. Vickey[142], O.E. Vickey Boeriu[142], G.H.A. Viehhauser[127], L. Vigani[62b], M. Vigl[110], M. Villa[24b,24a], M. Villaplana Perez[165], E.M. Villhauer[39], E. Vilucchi[52], M. Vincent[165], M.G. Vincter[35], A. Visibile[116], A. Visive[116], C. Vittori[24b,24a], I. Vivarelli[24b,24a], M.I. Vivas Albornoz[47], E. Voevodina[110], F. Vogel[109], J.C. Voigt[49], P. Vokac[133], Yu. Volkotrub[85b], L. Vomberg[25], E. Von Toerne[25], B. Vormwald[37], K. Vorobev[50], M. Vos[165], K. Voss[144], M. Vozak[37], L. Vozdecky[121], N. Vranjes[16], M. Vranjes Milosavljevic[16], M. Vreeswijk[116], N.K. Vu[112a], R. Vuillermet[37], I. Vukotic[39], I. K. Vyas[35], J.F. Wack[33], A. Wada[111], S. Wada[160], C. Wagner[146], J.M. Wagner[18a], W. Wagner[173], S. Wahdan[173], H. Wahlberg[90], C. H. Waits[121], J. Walder[135], R. Walker[109], K. Walkingshaw Pass[58], W. Walkowiak[144], A. Wall[129], E.J. Wallin[98], T. Wamorkar[146], K. Wandall-Christensen[165], A. Wang[61], A.Z. Wang[137], C. Wang[47], C. Wang[11], H. Wang[18a], J. Wang[63c], P. Wang[101], P. Wang[96], R. Wang[60], R. Wang[106], R. Wang[6], S. Wang[14,ar], S.M. Wang[151],

JHEP10(2026)027

T. Wang[115], T. Wang[61], W. Wang[113c], W.T. Wang[127], X. Wang[164], X. Wang[141a], X. Wang[47], Y. Wang[148], Y. Wang[114], Z. Wang[14], Z. Wang[63b], C. Wanotayaroj[82], A. Warburton[104], A.L. Warnerbring[144], S. Waterhouse[96], A.T. Watson[21], H. Watson[51], M.F. Watson[21], E. Watton[37], G. Watts[140], B.M. Waugh[96], J. M. Webb[53], C. Weber[30], M.S. Weber[20], C. Wei[61], Y. Wei[53], A.R. Weidberg[127], E.J. Weik[118], J. Weingarten[48], C. Weiser[53], C.J. Wells[47], P.S. Wells[37], T. Wenaus[30], T. Wengler[37], N.S. Wenke[110], N. Wermes[25], D. Werner[47], M. Wessels[62a], A.M. Wharton[91], A. White[8], A.S. White[37], M.J. White[1], D. Whiteson[162], W. Wiedenmann[172], M. Wielers[135], R. Wierda[147], C. Wiglesworth[42], H.G. Wilkens[37], J. J. H. Wilkinson[33], S. Williams[33], S. Willocq[103], D.J. Wilson[101], P.J. Windischhofer[39], F.I. Winkel[31], F. Winklmeier[124], B.T. Winter[53], M. Wittgen[146], M. Wobisch[97], T. Wojtkowski[59], Z. Wolffs[116], J. Wollrath[37], M.W. Wolter[86], H. Wolters[131a,131c], M.C. Wong[137], E.L. Woodward[41], S.D. Worm[47], B.K. Wosiek[86], K. A. Wozniak[55], K.W. Woźniak[86], S. Wozniewski[54], K. Wraight[58], C. Wu[158], J. Wu[156], M. Wu[112b], M. Wu[115], S. Wu[14,ar], S.L. Wu[172], X. Wu[61], Y. Wu[61], Y.Q. Wu[158], Z. Wu[102], Z. Wu[112a], J. Wuerzinger[110], T.R. Wyatt[101], B.M. Wynne[51], S. Xella[42], L. Xia[112a], M. Xie[61], A. Xiong[124], I. Xiotidis[37], D. Xu[14], H. Xu[61], L. Xu[61], R. Xu[129], T. Xu[106], W. Xu[112a], Y. Xu[140], Z. Xu[51], R. Xue[130], B. Yabsley[150], S. Yacoob[11], Y. Yamaguchi[82], E. Yamashita[156], H. Yamauchi[160], T. Yamazaki[18a], Y. Yamazaki[84], F. Yan[2], S. Yan[58], Z. Yan[103], C. Yang[18a], H.J. Yang[141a], H.T. Yang[61], S. Yang[61], X. Yang[37], X. Yang[14], Y. Yang[156], Y. Yang[61], W-M. Yao[18a], C. L. Yardley[149], J. Ye[14], S. Ye[30], X. Ye[106], I. Yeletskikh[38], B. Yeo[18b], M.R. Yexley[96], T. P. Yildirim[127], K. Yorita[156], C. Young[146], C.J.S. Young[37], I.N.L. Young[58], N.D. Young[124], D. Yu[141b,5], Y. Yu[61], J. Yuan[14,112c,ar], M. Yuan[106], R. Yuan[141b], L. Yue[96], M. Zaazoua[61], B. Zabinski[86], I. Zahir[36a], Q.U.A. Zahoor[51], A. Zaio[56b,56a], Z.K. Zak[86], T. Zakareishvili[165], S. Zambito[55], J. Zang[156], R. Zanzottera[70a,70b], O. Zaplatilek[133], I. Zatocilova[53], E. Zaya[147], C. Zeitnitz[173], H. Zeng[14], D.T. Zenger Jr[27], T. Ženiš[29a], S. Zenz[94], W. Zhan[61], B. Zhang[169], D.F. Zhang[142], G. Zhang[14,ar], J. Zhang[113b], J. Zhang[6], L. Zhang[61], L. Zhang[112a], P. Zhang[14,112c], R. Zhang[112a], S. Zhang[14], Y. Zhang[140], Y. Zhang[96], Y. Zhang[61], Y. Zhang[112a], Z. Zhang[149], Z. Zhang[101], Z. Zhang[18a], Z. Zhang[113b], Z. Zhang[65], H. Zhao[140], T. Zhao[113b], Y. Zhao[35], Z. Zhao[61], Z. Zhao[61], A. Zhemchugov[38], J. Zheng[112a], K. Zheng[164], L. Zheng[113b], X. Zheng[61], Z. Zheng[146], D. Zhong[164], B. Zhou[106], B. Zhou[141b,141a], N. Zhou[141a], Y. Zhou[15], Y. Zhou[112a], Y. Zhou[7], Z. Zhou[61], J. Zhu[106], X. Zhu[141b], Y. Zhu[141a], X. Zhuang[14], K. Zhukov[67], P. Ziakas[4], N.I. Zimine[38], J. Zinsser[62b], M. Ziolkowski[144], L. Živković[16], A. Zoccoli[24b,24a], K. Zoch[37], A. Zografos[37], T.G. Zorbas[142], L. Zwalinski[37]

[1] *Department of Physics, University of Adelaide, Adelaide, Australia*
[2] *Department of Physics, University of Alberta, Edmonton AB, Canada*
[3a] *Department of Physics, Ankara University, Ankara, Türkiye*
[3b] *Division of Physics, TOBB University of Economics and Technology, Ankara, Türkiye*
[4] *LAPP, Université Savoie Mont Blanc, CNRS/IN2P3, Annecy, France*
[5] *APC, Université Paris Cité, CNRS/IN2P3, Paris, France*
[6] *High Energy Physics Division, Argonne National Laboratory, Argonne IL, U.S.A.*
[7] *Department of Physics, University of Arizona, Tucson AZ, U.S.A.*
[8] *Department of Physics, University of Texas at Arlington, Arlington TX, U.S.A.*

JHEP10(2026)027

[9] Physics Department, National and Kapodistrian University of Athens, Athens, Greece
[10] Physics Department, National Technical University of Athens, Zografou, Greece
[11] Department of Physics, University of Texas at Austin, Austin TX, U.S.A.
[12] Institute of Physics, Azerbaijan Academy of Sciences, Baku, Azerbaijan
[13] Institut de Física d'Altes Energies (IFAE), Barcelona Institute of Science and Technology, Barcelona, Spain
[14] Institute of High Energy Physics, Chinese Academy of Sciences, Beijing, China
[15] Physics Department, Tsinghua University, Beijing, China
[16] Institute of Physics, University of Belgrade, Belgrade, Serbia
[17] Department for Physics and Technology, University of Bergen, Bergen, Norway
[18a] Physics Division, Lawrence Berkeley National Laboratory, Berkeley CA, U.S.A.
[18b] University of California, Berkeley CA, U.S.A.
[19] Institut für Physik, Humboldt Universität zu Berlin, Berlin, Germany
[20] Albert Einstein Center for Fundamental Physics and Laboratory for High Energy Physics, University of Bern, Bern, Switzerland
[21] School of Physics and Astronomy, University of Birmingham, Birmingham, U.K.
[22a] Department of Physics, Bogazici University, Istanbul, Türkiye
[22b] Department of Physics Engineering, Gaziantep University, Gaziantep, Türkiye
[22c] Department of Physics, Istanbul University, Istanbul, Türkiye
[23a] Facultad de Ciencias y Centro de Investigaciónes, Universidad Antonio Nariño, Bogotá, Colombia
[23b] Departamento de Física, Universidad Nacional de Colombia, Bogotá, Colombia
[24a] Dipartimento di Fisica e Astronomia A. Righi, Università di Bologna, Bologna, Italy
[24b] INFN Sezione di Bologna, Italy
[25] Physikalisches Institut, Universität Bonn, Bonn, Germany
[26] Department of Physics, Boston University, Boston MA, U.S.A.
[27] Department of Physics, Brandeis University, Waltham MA, U.S.A.
[28a] Transilvania University of Brasov, Brasov, Romania
[28b] Horia Hulubei National Institute of Physics and Nuclear Engineering, Bucharest, Romania
[28c] Department of Physics, Alexandru Ioan Cuza University of Iasi, Iasi, Romania
[28d] National Institute for Research and Development of Isotopic and Molecular Technologies, Physics Department, Cluj-Napoca, Romania
[28e] National University of Science and Technology Politechnica, Bucharest, Romania
[28f] West University in Timisoara, Timisoara, Romania
[28g] Faculty of Physics, University of Bucharest, Bucharest, Romania
[29a] Faculty of Mathematics, Physics and Informatics, Comenius University, Bratislava, Slovak Republic
[29b] Department of Subnuclear Physics, Institute of Experimental Physics of the Slovak Academy of Sciences, Kosice, Slovak Republic
[30] Physics Department, Brookhaven National Laboratory, Upton NY, U.S.A.
[31] Universidad de Buenos Aires, Facultad de Ciencias Exactas y Naturales, Departamento de Física, y CONICET, Instituto de Física de Buenos Aires (IFIBA), Buenos Aires, Argentina
[32] California State University, CA, U.S.A.
[33] Cavendish Laboratory, University of Cambridge, Cambridge, U.K.
[34a] Department of Physics, University of Cape Town, Cape Town, South Africa
[34b] iThemba Labs, Western Cape, South Africa
[34c] Department of Mechanical Engineering Science, University of Johannesburg, Johannesburg, South Africa
[34d] National Institute of Physics, University of the Philippines Diliman (Philippines), Philippines
[34e] Department of Physics, Stellenbosch University, Matieland, South Africa
[34f] University of KwaZulu-Natal, School of Agriculture and Science, Mathematics, Westville, South Africa
[34g] University of South Africa, Department of Physics, Pretoria, South Africa
[34h] University of Pretoria, Department of Mechanical and Aeronautical Engineering, Pretoria, South Africa
[34i] University of Zululand, KwaDlangezwa, South Africa
[34j] School of Physics, University of the Witwatersrand, Johannesburg, South Africa
[35] Department of Physics, Carleton University, Ottawa ON, Canada

JHEP10(2026)027

[36a] Faculté des Sciences Ain Chock, Université Hassan II de Casablanca, Morocco
[36b] Faculté des Sciences, Université Ibn-Tofail, Kénitra, Morocco
[36c] Faculté des Sciences Semlalia, Université Cadi Ayyad, LPHEA-Marrakech, Morocco
[36d] LPMR, Faculté des Sciences, Université Mohamed Premier, Oujda, Morocco
[36e] Faculté des sciences, Université Mohammed V, Rabat, Morocco
[36f] Institute of Applied Physics, Mohammed VI Polytechnic University, Ben Guerir, Morocco
[37] CERN, Geneva, Switzerland
[38] Affiliated with an international laboratory covered by a cooperation agreement with CERN
[39] Enrico Fermi Institute, University of Chicago, Chicago IL, U.S.A.
[40] LPC, Université Clermont Auvergne, CNRS/IN2P3, Clermont-Ferrand, France
[41] Nevis Laboratory, Columbia University, Irvington NY, U.S.A.
[42] Niels Bohr Institute, University of Copenhagen, Copenhagen, Denmark
[43a] Dipartimento di Fisica, Università della Calabria, Rende, Italy
[43b] INFN Gruppo Collegato di Cosenza, Laboratori Nazionali di Frascati, Italy
[44] Physics Department, Southern Methodist University, Dallas TX, U.S.A.
[45] National Centre for Scientific Research "Demokritos", Agia Paraskevi, Greece
[46a] Department of Physics, Stockholm University, Sweden
[46b] Oskar Klein Centre, Stockholm, Sweden
[47] Deutsches Elektronen-Synchrotron DESY, Hamburg and Zeuthen, Germany
[48] Fakultät Physik, Technische Universität Dortmund, Dortmund, Germany
[49] Institut für Kern- und Teilchenphysik, Technische Universität Dresden, Dresden, Germany
[50] Department of Physics, Duke University, Durham NC, U.S.A.
[51] SUPA — School of Physics and Astronomy, University of Edinburgh, Edinburgh, U.K.
[52] INFN e Laboratori Nazionali di Frascati, Frascati, Italy
[53] Physikalisches Institut, Albert-Ludwigs-Universität Freiburg, Freiburg, Germany
[54] II. Physikalisches Institut, Georg-August-Universität Göttingen, Göttingen, Germany
[55] Département de Physique Nucléaire et Corpusculaire, Université de Genève, Genève, Switzerland
[56a] Dipartimento di Fisica, Università di Genova, Genova, Italy
[56b] INFN Sezione di Genova, Italy
[57] II. Physikalisches Institut, Justus-Liebig-Universität Giessen, Giessen, Germany
[58] SUPA — School of Physics and Astronomy, University of Glasgow, Glasgow, U.K.
[59] LPSC, Université Grenoble Alpes, CNRS/IN2P3, Grenoble INP, Grenoble, France
[60] Laboratory for Particle Physics and Cosmology, Harvard University, Cambridge MA, U.S.A.
[61] Department of Modern Physics and State Key Laboratory of Particle Detection and Electronics, University of Science and Technology of China, Hefei, China
[62a] Kirchhoff-Institut für Physik, Ruprecht-Karls-Universität Heidelberg, Heidelberg, Germany
[62b] Physikalisches Institut, Ruprecht-Karls-Universität Heidelberg, Heidelberg, Germany
[63a] Department of Physics, Chinese University of Hong Kong, Shatin, N.T., Hong Kong, China
[63b] Department of Physics, University of Hong Kong, Hong Kong, China
[63c] Department of Physics and Institute for Advanced Study, Hong Kong University of Science and Technology, Clear Water Bay, Kowloon, Hong Kong, China
[64] Department of Physics, National Tsing Hua University, Hsinchu, Taiwan
[65] IJCLab, Université Paris-Saclay, CNRS/IN2P3, 91405, Orsay, France
[66] Centro Nacional de Microelectrónica (IMB-CNM-CSIC), Barcelona, Spain
[67] Department of Physics, Indiana University, Bloomington IN, U.S.A.
[68a] INFN Gruppo Collegato di Udine, Sezione di Trieste, Udine, Italy
[68b] ICTP, Trieste, Italy
[68c] Dipartimento Politecnico di Ingegneria e Architettura, Università di Udine, Udine, Italy
[69a] INFN Sezione di Lecce, Italy
[69b] Dipartimento di Matematica e Fisica, Università del Salento, Lecce, Italy
[70a] INFN Sezione di Milano, Italy
[70b] Dipartimento di Fisica, Università di Milano, Milano, Italy
[71a] INFN Sezione di Napoli, Italy

JHEP10(2026)027

[71b] *Dipartimento di Fisica, Università di Napoli, Napoli, Italy*
[72a] *INFN Sezione di Pavia, Italy*
[72b] *Dipartimento di Fisica, Università di Pavia, Pavia, Italy*
[73a] *INFN Sezione di Pisa, Italy*
[73b] *Dipartimento di Fisica E. Fermi, Università di Pisa, Pisa, Italy*
[74a] *INFN Sezione di Roma, Italy*
[74b] *Dipartimento di Fisica, Sapienza Università di Roma, Roma, Italy*
[75a] *INFN Sezione di Roma Tor Vergata, Italy*
[75b] *Dipartimento di Fisica, Università di Roma Tor Vergata, Roma, Italy*
[76a] *INFN Sezione di Roma Tre, Italy*
[76b] *Dipartimento di Matematica e Fisica, Università Roma Tre, Roma, Italy*
[77a] *INFN-TIFPA, Italy*
[77b] *Università degli Studi di Trento, Trento, Italy*
[78] *Universität Innsbruck, Department of Astro and Particle Physics, Innsbruck, Austria*
[79] *Department of Physics and Astronomy, Iowa State University, Ames IA, U.S.A.*
[80] *Istinye University, Sariyer, Istanbul, Türkiye*
[81a] *Departamento de Engenharia Elétrica, Universidade Federal de Juiz de Fora (UFJF), Juiz de Fora, Brazil*
[81b] *Universidade Federal do Rio De Janeiro COPPE/EE/IF, Rio de Janeiro, Brazil*
[81c] *Instituto de Física, Universidade de São Paulo, São Paulo, Brazil*
[81d] *Rio de Janeiro State University, Rio de Janeiro, Brazil*
[81e] *Federal University of Bahia, Bahia, Brazil*
[82] *KEK, High Energy Accelerator Research Organization, Tsukuba, Japan*
[83a] *Khalifa University of Science and Technology, Abu Dhabi, United Arab Emirates*
[83b] *New York University Abu Dhabi, Abu Dhabi, United Arab Emirates*
[83c] *United Arab Emirates University, Al Ain, United Arab Emirates*
[83d] *University of Sharjah, Sharjah, United Arab Emirates*
[84] *Graduate School of Science, Kobe University, Kobe, Japan*
[85a] *AGH University of Krakow, Faculty of Physics and Applied Computer Science, Krakow, Poland*
[85b] *Marian Smoluchowski Institute of Physics, Jagiellonian University, Krakow, Poland*
[86] *Institute of Nuclear Physics Polish Academy of Sciences, Krakow, Poland*
[87] *Faculty of Science, Kyoto University, Kyoto, Japan*
[88] *Research Center for Advanced Particle Physics and Department of Physics, Kyushu University, Fukuoka, Japan*
[89] *L2IT, Université de Toulouse, CNRS/IN2P3, UPS, Toulouse, France*
[90] *Instituto de Física La Plata, Universidad Nacional de La Plata and CONICET, La Plata, Argentina*
[91] *Physics Department, Lancaster University, Lancaster, U.K.*
[92] *Oliver Lodge Laboratory, University of Liverpool, Liverpool, U.K.*
[93] *Department of Experimental Particle Physics, Jožef Stefan Institute and Department of Physics, University of Ljubljana, Ljubljana, Slovenia*
[94] *Department of Physics and Astronomy, Queen Mary University of London, London, U.K.*
[95] *Department of Physics, Royal Holloway University of London, Egham, U.K.*
[96] *Department of Physics and Astronomy, University College London, London, U.K.*
[97] *Louisiana Tech University, Ruston LA, U.S.A.*
[98] *Fysiska institutionen, Lunds universitet, Lund, Sweden*
[99] *Departamento de Física Teorica C-15 and CIAFF, Universidad Autónoma de Madrid, Madrid, Spain*
[100] *Institut für Physik, Universität Mainz, Mainz, Germany*
[101] *School of Physics and Astronomy, University of Manchester, Manchester, U.K.*
[102] *CPPM, Aix-Marseille Université, CNRS/IN2P3, Marseille, France*
[103] *Department of Physics, University of Massachusetts, Amherst MA, U.S.A.*
[104] *Department of Physics, McGill University, Montreal QC, Canada*
[105] *School of Physics, University of Melbourne, Victoria, Australia*
[106] *Department of Physics, University of Michigan, Ann Arbor MI, U.S.A.*
[107] *Department of Physics and Astronomy, Michigan State University, East Lansing MI, U.S.A.*

JHEP10(2026)027

[108] Group of Particle Physics, University of Montreal, Montreal QC, Canada
[109] Fakultät für Physik, Ludwig-Maximilians-Universität München, München, Germany
[110] Max-Planck-Institut für Physik (Werner-Heisenberg-Institut), München, Germany
[111] Graduate School of Science and Kobayashi-Maskawa Institute, Nagoya University, Nagoya, Japan
[112a] Department of Physics, Nanjing University, Nanjing, China
[112b] School of Science, Shenzhen Campus of Sun Yat-sen University, China
[112c] University of Chinese Academy of Science (UCAS), Beijing, China
[113a] School of Physics, Nankai University, Tianjin, China
[113b] Institute of Frontier and Interdisciplinary Science and Key Laboratory of Particle Physics and Particle Irradiation (MOE), Shandong University, Qingdao, China
[113c] School of Physics, Zhengzhou University, China
[114] Department of Physics and Astronomy, University of New Mexico, Albuquerque NM, U.S.A.
[115] Institute for Mathematics, Astrophysics and Particle Physics, Radboud University/Nikhef, Nijmegen, Netherlands
[116] Nikhef National Institute for Subatomic Physics and University of Amsterdam, Amsterdam, Netherlands
[117] Department of Physics, Northern Illinois University, DeKalb IL, U.S.A.
[118] Department of Physics, New York University, New York NY, U.S.A.
[119] Ochanomizu University, Otsuka, Bunkyo-ku, Tokyo, Japan
[120] Ohio State University, Columbus OH, U.S.A.
[121] Homer L. Dodge Department of Physics and Astronomy, University of Oklahoma, Norman OK, U.S.A.
[122] Department of Physics, Oklahoma State University, Stillwater OK, U.S.A.
[123] Palacký University, Joint Laboratory of Optics, Olomouc, Czech Republic
[124] Institute for Fundamental Science, University of Oregon, Eugene, OR, U.S.A.
[125] Graduate School of Science, University of Osaka, Osaka, Japan
[126] Department of Physics, University of Oslo, Oslo, Norway
[127] Department of Physics, Oxford University, Oxford, U.K.
[128] LPNHE, Sorbonne Université, Université Paris Cité, CNRS/IN2P3, Paris, France
[129] Department of Physics, University of Pennsylvania, Philadelphia PA, U.S.A.
[130] Department of Physics and Astronomy, University of Pittsburgh, Pittsburgh PA, U.S.A.
[131a] Laboratório de Instrumentação e Física Experimental de Partículas — LIP, Lisboa, Portugal
[131b] Departamento de Física, Faculdade de Ciências, Universidade de Lisboa, Lisboa, Portugal
[131c] Departamento de Física, Universidade de Coimbra, Coimbra, Portugal
[131d] Centro de Física Nuclear da Universidade de Lisboa, Lisboa, Portugal
[131e] Departamento de Física, Escola de Ciências, Universidade do Minho, Braga, Portugal
[131f] Departamento de Física Teórica y del Cosmos, Universidad de Granada, Granada (Spain), Spain
[131g] Departamento de Física, Instituto Superior Técnico, Universidade de Lisboa, Lisboa, Portugal
[132] Institute of Physics of the Czech Academy of Sciences, Prague, Czech Republic
[133] Czech Technical University in Prague, Prague, Czech Republic
[134] Charles University, Faculty of Mathematics and Physics, Prague, Czech Republic
[135] Particle Physics Department, Rutherford Appleton Laboratory, Didcot, U.K.
[136] IRFU, CEA, Université Paris-Saclay, Gif-sur-Yvette, France
[137] Santa Cruz Institute for Particle Physics, University of California Santa Cruz, Santa Cruz CA, U.S.A.
[138a] Departamento de Física, Pontificia Universidad Católica de Chile, Santiago, Chile
[138b] Millennium Institute for Subatomic physics at high energy frontier (SAPHIR), Santiago, Chile
[138c] Instituto de Investigación Multidisciplinario en Ciencia y Tecnología, y Departamento de Física, Universidad de La Serena, Chile
[138d] Universidad Andres Bello, Department of Physics, Santiago, Chile
[138e] Universidad San Sebastian, Recoleta, Chile
[138f] Instituto de Alta Investigación, Universidad de Tarapacá, Arica, Chile
[138g] Departamento de Física, Universidad Técnica Federico Santa María, Valparaíso, Chile
[139] Department of Physics, Institute of Science, Tokyo, Japan
[140] Department of Physics, University of Washington, Seattle WA, U.S.A.

JHEP10(2026)027

[141a] State Key Laboratory of Dark Matter Physics, School of Physics and Astronomy, Shanghai Jiao Tong University, Key Laboratory for Particle Astrophysics and Cosmology (MOE), SKLPPC, Shanghai, China
[141b] State Key Laboratory of Dark Matter Physics, Tsung-Dao Lee Institute, Shanghai Jiao Tong University, Shanghai, China
[142] Department of Physics and Astronomy, University of Sheffield, Sheffield, U.K.
[143] Department of Physics, Shinshu University, Nagano, Japan
[144] Department Physik, Universität Siegen, Siegen, Germany
[145] Department of Physics, Simon Fraser University, Burnaby BC, Canada
[146] SLAC National Accelerator Laboratory, Stanford CA, U.S.A.
[147] Department of Physics, Royal Institute of Technology, Stockholm, Sweden
[148] Departments of Physics and Astronomy, Stony Brook University, Stony Brook NY, U.S.A.
[149] Department of Physics and Astronomy, University of Sussex, Brighton, U.K.
[150] School of Physics, University of Sydney, Sydney, Australia
[151] Institute of Physics, Academia Sinica, Taipei, Taiwan
[152a] E. Andronikashvili Institute of Physics, Iv. Javakhishvili Tbilisi State University, Tbilisi, Georgia
[152b] High Energy Physics Institute, Tbilisi State University, Tbilisi, Georgia
[152c] University of Georgia, Tbilisi, Georgia
[153] Department of Physics, Technion, Israel Institute of Technology, Haifa, Israel
[154] Raymond and Beverly Sackler School of Physics and Astronomy, Tel Aviv University, Tel Aviv, Israel
[155] Department of Physics, Aristotle University of Thessaloniki, Thessaloniki, Greece
[156] International Center for Elementary Particle Physics and Department of Physics, University of Tokyo, Tokyo, Japan
[157] Graduate School of Science and Technology, Tokyo Metropolitan University, Tokyo, Japan
[158] Department of Physics, University of Toronto, Toronto ON, Canada
[159a] TRIUMF, Vancouver BC, Canada
[159b] Department of Physics and Astronomy, York University, Toronto ON, Canada
[160] Division of Physics and Tomonaga Center for the History of the Universe, Faculty of Pure and Applied Sciences, University of Tsukuba, Tsukuba, Japan
[161] Department of Physics and Astronomy, Tufts University, Medford MA, U.S.A.
[162] Department of Physics and Astronomy, University of California Irvine, Irvine CA, U.S.A.
[163] Department of Physics and Astronomy, University of Uppsala, Uppsala, Sweden
[164] Department of Physics, University of Illinois, Urbana IL, U.S.A.
[165] Instituto de Física Corpuscular (IFIC), Centro Mixto Universidad de Valencia — CSIC, Valencia, Spain
[166] Department of Physics, University of British Columbia, Vancouver BC, Canada
[167] Department of Physics and Astronomy, University of Victoria, Victoria BC, Canada
[168] Fakultät für Physik und Astronomie, Julius-Maximilians-Universität Würzburg, Würzburg, Germany
[169] Department of Physics, University of Warwick, Coventry, U.K.
[170] Waseda University, Tokyo, Japan
[171] Department of Particle Physics and Astrophysics, Weizmann Institute of Science, Rehovot, Israel
[172] Department of Physics, University of Wisconsin, Madison WI, U.S.A.
[173] Fakultät für Mathematik und Naturwissenschaften, Fachgruppe Physik, Bergische Universität Wuppertal, Wuppertal, Germany
[174] Department of Physics, Yale University, New Haven CT, U.S.A.
[175] Yerevan Physics Institute, Yerevan, Armenia

[a] Also at Department of Physics, King's College London, London, U.K.
[b] Also at Institute of Physics, Azerbaijan Academy of Sciences, Baku, Azerbaijan
[c] Also at Imam Mohammad Ibn Saud Islamic University, Saudi Arabia
[d] Also at Department of Physics, University of Thessaly, Greece
[e] Also at Département de Physique Nucléaire et Corpusculaire, Université de Genève, Genève, Switzerland
[f] Also at An-Najah National University, Nablus, Palestine
[g] Also at Department of Physics, University of Fribourg, Fribourg, Switzerland
[h] Also at Department of Physics, Westmont College, Santa Barbara, U.S.A.

JHEP10(2026)027

[i] Also at Departament de Fisica de la Universitat Autonoma de Barcelona, Barcelona, Spain
[j] Also at University of Siena, Italy
[k] Also at Affiliated with an institute formerly covered by a cooperation agreement with CERN
[l] Also at The Collaborative Innovation Center of Quantum Matter (CICQM), Beijing, China
[m] Also at Faculty of Physics, Sofia University, 'St. Kliment Ohridski', Sofia, Bulgaria
[n] Also at Università di Napoli Parthenope, Napoli, Italy
[o] Also at Institute of Particle Physics (IPP), Canada
[p] Also at Department of Physics, Bolu Abant Izzet Baysal University, Bolu, Türkiye
[q] Also at Faculty of Physics, University of Bucharest, Romania
[r] Also at Borough of Manhattan Community College, City University of New York, New York NY, U.S.A.
[s] Also at National Institute of Physics, University of the Philippines Diliman (Philippines), Philippines
[t] Also at TRIUMF, Vancouver BC, Canada
[u] Also at Universita degli Studi Link, Italy
[v] Also at Department of Financial and Management Engineering, University of the Aegean, Chios, Greece
[w] Also at University and INFN Torino, Torino, Italy
[x] Also at Institucio Catalana de Recerca i Estudis Avancats, ICREA, Barcelona, Spain
[y] Also at Henan University, China
[z] Also at Yeditepe University, Physics Department, Istanbul, Türkiye
[aa] Also at Institute of Theoretical Physics, Ilia State University, Tbilisi, Georgia
[ab] Also at CERN, Geneva, Switzerland
[ac] Also at Center for Interdisciplinary Research and Innovation (CIRI-AUTH), Thessaloniki, Greece
[ad] Also at Hellenic Open University, Patras, Greece
[ae] Also at Department of Modern Physics and State Key Laboratory of Particle Detection and Electronics, University of Science and Technology of China, Hefei, China
[af] Also at Department of Physics, Stellenbosch University, South Africa
[ag] Also at School of Physics, University of the Witwatersrand, Johannesburg, South Africa
[ah] Also at Department of Physics, Ben Gurion University of the Negev, Beer Sheva, Israel
[ai] Also at University of Colorado Boulder, Department of Physics, Colorado, U.S.A.
[aj] Also at Centre of Physics of the Universities of Minho and Porto (CF-UM-UP), Portugal
[ak] Also at Indian Institute of Technology (IIT), Jodhpur, India
[al] Also at Institute for Nuclear Research and Nuclear Energy (INRNE) of the Bulgarian Academy of Sciences, Sofia, Bulgaria
[am] Also at Washington College, Chestertown, MD, U.S.A.
[an] Also at Institut für Experimentalphysik, Universität Hamburg, Hamburg, Germany
[ao] Also at Institute of Applied Physics, Mohammed VI Polytechnic University, Ben Guerir, Morocco
[ap] Also at Institute of Physics and Technology, Mongolian Academy of Sciences, Ulaanbaatar, Mongolia
[aq] Also at Millennium Institute for Subatomic physics at high energy frontier (SAPHIR), Santiago, Chile
[ar] Also at University of Chinese Academy of Sciences (UCAS), Beijing, China
[†] Deceased

JHEP10(2026)027